(a) Distance estimated from the photometry.
(b) Calculated from V and $< m - M >_{binary}$=3.40
(1) ADS 2451. The photometry include the visual companion. Mason et al. (1993) estimated $\Delta V=6.0^m$.
(2) Distance and spectral types from Strassmeier et al 1993. $(B\text{-}V)_p$ was assigned according the espectral type.
(3) $\Delta V=1.75^m$ from Griffin & Gunn (1981). Probable triple system.
(4) $\Delta V=0.5^m$ from Griffin & Gunn (1981).
(5) $(B\text{-}V)_p$ measured directly during the eclipse (Schiller & Milone 1987).
(6) $\Delta V=0.35^m$ from Batten & Wallerstein (1973). It could have an additional component.
(7) $\Delta V=1.12^m$ from Griffin et al. (1982).
(8) ADS 3135. $\Delta V=1.0^m$ from Wickes (1975). V={7.24+8.24} from Peterson & Solenski (1987). Visual companion included in the photometry.
(9) Boesgaard & Tripicco (1986) obtained $\Delta V=0.056^m$ from the ratio between spectral lines.
(10) Visual component included in the photometry.
(11) ADS 3169. Visual component included in the photometry.
(12) The contribution from the secondary is apparently negligible.
(13) The contribution from the secondary is apparently negligible.
(14) $\Delta V=2.0^m$ from Griffin et al. (1985).
(15) $\Delta V=0.45^m$ from Peterson & Solenski (1987). V={7.01+7.46}. The visual companion is included in the photometry.
(16) ADS 3210. $\Delta V=0.50^m$ from Heintz (1969). V={8.06+8.56} from Peterson & Solenski (1987). The visual companion is included in the photometry.
(17) V_{obs}=9.03 from Mermilliod (1976).
(18) ADS 3248. $\Delta V=0.65^m$ from Dombrowski (1991). Triple system. The inner pair is the SB2.
The whole deconvolution is {F7 V + K0 V} + F9 V, V = {3.644 + 5.655} + 4.136, (B-V) = {0.481 + 0.819} + 0.545
(19) The contribution from the secondary is apparently negligible.
(20) The visual companion is *not* included in the photometry.
(21) Strassmeier et al. (1993) give $M_V = 6.8^m$, D=16.7 pc and dK5e. Apparent magnitude from Eggen & Greenstein (1965). Distance from Borgman & Lippicott (1983). Another possibility for the deconvolution could be $(B\text{-}V)_{calc}$=1.085, $(B\text{-}V)_p$=1.068, $(B\text{-}V)_s$=1.7, M_{calc}=6.648, M_p=6.687, M_s=10.291, $(1+\alpha)$=1.036, $\Delta V=3.6^m$.
(22) ΔV=2.0, Griffin et al. (1985).
(23) The deconvolution was taken from Griffin et al. (1985).
(24) The contribution from the secondary is apparently negligible.
(25) $\Delta V=0.14^m$, Spectral types, distance and deconvolution from Griffin et al. (1985).
(26) $V_{primary}$=10.28, $V_{secondary}$=10.59, Griffin & Gunn (1978). Distance from Schwan (1991), Spectral types from Strassmeier et al. (1993)
(27) $\Delta V=0.2^m$ from Thorburn et al. (1993) from the ratio between CaI 6718Å. V_{obs}=7.34, 7.59, 7.71, 7.73 and 8.18, from Schwan (1991), Mermilliod (1976), Stern (1994) and Mason et al. (1993), respectively.
(28) ADS 3475. Also $(B\text{-}V)_{obs}$=0.50 from Mermilliod (1976). $\Delta V=0.19^m$ from Dombrowski (1991). The visual component is included in the photometry.
(29) ADS 3483. Triple system (Griffin et al. 1985):
{F5 V + G8 V} + G4 V, V = {3.4 + 5.58} + 4.96, (B-V) = {0.42 + 0.81} + 0.68

Table 1: Deconvolution for the Hyades binaries. The photometry is essentially from Johnson & Knuckles (1955) and the distances from Stern (1994). Spectral types for the primary and secondary components were assigned from (B-V) color indices by using the Schmidt–Kaler's (1982) ZAMS.

Star	(B-V)			Dist.	M_V			V_{obs}	Sp. Type			Binarity
	Obs.	Prim.	Sec.	(pc)	Obs.	Prim.	Sec.		Obs.	Prim.	Sec.	
(1)	(2)	(3)	(4)	(5)	(6)	(7)	(8)	(9)	(10)	(11)	(12)	(13)
vB 1[(1)]	0.566	0.559	1.448	43.1	4.228	4.241	9.028	7.40	–	F9 V	M1 V	VB
V471 Tau[(2)]	0.85	∼0.993	–	59	5.86	5.35	9.75	9.71	–	K2 V	WD	SB1
vB 9	0.708	–	–	(47.9)[(b)]	5.27[(b)]	–	–	8.67	–	G6 V	–	SB1
vB 14	0.355	0.350	1.337	38.3	2.814	2.822	8.141	5.73	–	F2 V	K8 V	SB
BD+23°635[(3)]	1.09	1.043	1.362	(39.9)[(a)]	6.375	6.573	8.322	9.38	–	K3.5 V	K9 V	SB2
vB 162[(4)]	0.705	0.666	0.746	49.1	4.375	4.934	5.283	7.83	–	G4 V	G9 V	SB2
vB 22[(5)]	0.771	0.713	0.945	50.8	4.811	5.155	6.226	8.34	G8 V	G6 V	K3 V	SB2
vB 23[(6)]	0.679	0.654	0.714	49.3	4.076	4.815	5.161	7.54	–	G3 V	G6 V	SB2
BD+22°669[(7)]	0.99	0.933	1.167	(53.1)[(a)]	5.859	6.190	7.310	9.48	K0	K2 V	K5 V	SB2
vB 29[(8)]	0.561	0.520	0.670	47.3	3.506	3.898	4.896	6.88	F8 V	F8 V	G5 V	SB
vB 34[(9)]	0.457	0.435	0.461	50.3	2.662	3.456	3.506	6.17	F6 V	F5 V	F6 V	SB2
vB 38[(10)]	0.320	0.296	0.764	47.6	2.332	2.402	5.350	5.72	Am	F0 V	G9 V	SB1
vB 40[(11)]	0.563	0.528	1.042	41.9	3.879	3.974	6.567	6.99	G9 V	F9 V	K4 V	VB/SB1
vB 39[(12)]	0.678	0.678	–	38.2	4.950	4.950	–	7.86	–	G5 V	–	SB
vB 42	0.759	0.750	1.492	52.0	5.280	5.298	9.750	8.86	G9 V	G8 V	M2 V	PhB
vB 50	0.601	0.578	1.252	45.9	4.311	4.361	7.668	7.62	G1 V	G0 V	K6 V	SB
vB 52[(13)]	0.597	0.597	–	43.9	4.588	4.588	–	7.80	G1 V	G0 V	–	SB?
vB 140[(14)]	0.757	0.708	1.134	51.2	4.973	5.131	7.130	8.94	–	G6 V	K5 V	SB2
vB 57[(15)]	0.491	0.466	0.530	51.2	2.914	3.542	3.989	6.46	F7 V	F6 V	F8 V	VB/SB2
vB 58[(16)]	0.680	0.642	0.742	46.1	4.211	4.771	5.269	7.53	G6 V	G4 V	G8 V	VB/SB2
vB 59	0.543	0.540	1.492	47.9	4.088	4.094	9.739	7.49	F8 V	F9 V	M2 V	SB
vB 62	0.537	0.518	1.194	51.0	3.842	3.883	7.443	7.38	F8 V	F8 V	K5.5 V	SB1
vB 63	0.632	0.630	1.522	46.6	4.718	4.721	11.074	8.06	G5 V	G2 V	M3 V	VB/SB1
vB 178[(17)]	0.837	0.794	1.295	52.7	5.421	5.541	7.868	9.03	K0 V	K0 V	K6 V	SB?
vB 69	0.746	0.714	1.315	51.5	5.081	5.159	7.983	8.64	G8 V	G6 V	K7 V	SB1
vB 75[(18)]	0.531	0.481	0.545	52.0	3.010	3.644	4.136	6.59	F8 V	F7 V	F9 V	VB/SB3
vB 77	0.502	0.489	1.281	47.2	3.680	3.705	7.800	7.05	F7 V	F8 V	K6.5	SB1
vB 81	0.470	0.461	1.327	52.7	3.491	3.507	8.068	7.10	F6 V	F6 V	K7 V	SB
vB 181	1.167	1.122	1.426	49.4	6.851	7.050	8.793	10.32	K	K5 V	M1 V	PhB
vB 182	0.884	0.820	1.062	53.3	5.296	5.661	6.657	8.93	–	K0 V	K4 V	SB1
vA677[(19)]	1.23	1.23	–	43.6	7.833	7.833	–	11.03	K6 V	K6 V	–	SB1
vB 91	0.883	0.819	1.074	53.1	5.315	5.659	6.728	8.94	K1 V	K0 V	K4 V	VB/SB1
vB 96[(20)]	0.841	0.811	0.881	50.1	5.011	5.634	5.910	8.51	KO IV/V	K0 V	K2 V	VB/SB1
J301[(21)]	1.085	1.085	–	16.7	7.306	6.789	–	8.42	dK5e	K4 V	–	SB1
vB 102	0.603	0.576	1.190	44.7	4.288	4.351	7.411	7.54	G1 V	G0 V	K5.5 V	VB/SB1
J304[(22)]	1.15	1.109	1.451	(47.1)[(a)]	6.805	6.965	8.963	10.17	K5	K5 V	M1 V	SB1
vB 106	0.669	0.623	1.089	48.6	4.527	4.666	6.829	7.96	–	G1 V	K4 V	SB1
vB 185[(23)]	1.1	1.046	1.299	51.6	5.907	6.587	7.886	9.47	K3 V	K3 V	K7 V	SB2
vB 142	0.665	0.661	1.501	50.3	4.832	4.832	10.304	8.34	–	G4 V	M2 V	SB1
vB 113[(24)]	0.549	0.549	–	41.2	4.186	4.186	–	7.26	–	F9 V	–	SB1
vB 114	0.723	0.706	1.435	49.0	5.089	5.124	8.845	8.54	–	G6 V	M1 V	SB1
J331[(25)]	1.41	1.400	1.421	(43.3)[(a)]	7.938	8.616	8.767	11.12	–	K8.8 V	K9.2 V	SB2
vB 115	0.843	0.814	1.393	50.5	5.574	5.645	8.567	9.09	–	K0 V	M0 V	SB1
vB 117[(26)]	1.06	1.036	1.093	48.02	6.263	6.544	6.853	9.67	K3 V	K3 V	K3 V	SB2
vB 119	0.559	0.528	1.077	44.3	3.888	3.969	6.745	7.12	–	F9 V	K4 V	SB1
vB 120[(27)]	0.735	0.712	0.764	52.7	4.494	5.150	5.350	7.71	–	G6 V	G8 V	VB/SB2
vB 121	0.504	0.493	1.324	52.1	3.706	3.726	8.044	7.29	–	F8 V	K7 V	SB
vB 122[(28)]	0.541	0.531	0.553	52.0	3.346	4.009	4.198	6.76	–	F9 V	F9 V	VB/SB2
vB 124[(29)]	0.497	0.428	0.783	54.2	3.057	3.319	4.879	6.27	F5/G8	F5 V	G5 V	SB2

Table 2: Observational data for the late spectral type Hyades binaries. The EW are not corrected for the contribution to the continuum level by the companion.

Name	V	SNR	EW(FeI6678) (mÅ)	EW(CaI6718) (mÅ)	EW(Fe+Li) (mÅ)	EW(Li) (mÅ)	Comments
(1)	(2)	(3)	(4)	(5)	(6)	(7)	(8)
V471 Tau	9.71	140	223.2	183.7	228.9	218.8	(a)
vA677	11.03	110	282.1	291.3	24.9	10.7	(b)
J301	8.42	132	247.7	260.3	32.1	16.2	
J304	10.17	85	199.5	205.5	16.5	$\leq$5.0	
vB185(p)	9.47	115	162.1	145.4	16.0	$\leq$2.3	
vB185(s)	–	–	109.1	119.6	4.6	$\leq$1.2	
J331(p)	11.12	45	119.2	133.0	–	$\leq$5.0	
J331(s)	–	–	87.2	110.9	–	11.3	(c)
vB117(p)	9.67	125	145.8	195.3	8.8	$\leq$2.4	
vB117(s)	–	–	114.8	166.4	6.9	$\leq$1.1	

pwd

(a) $<\mathrm{EW(FeI6707}>_{(\mathrm{B-V})=0.85}$=13.8 mÅ.

(b) $<\mathrm{EW(FeI6707}>_{(\mathrm{B-V})=1.23}$=14.7 mÅ.

(c) $\mathrm{EW[Li(s)+Fe(p)]}^{\mathrm{measured}}$=24.3. Assumed $\mathrm{EW[Fe(p)]}^{\mathrm{corrected}}=\mathrm{EW[Fe(s)]}^{\mathrm{corrected}}$. $\mathrm{EW[Fe(s)]}^{\mathrm{measured}}$=11.4

(p) Primary component.

(s) Secondary component.

Table 3: Original abundances and corrections. The observed EW(Li) were taken primarily from Thorburn et al. (1993). The abundances commented with SCG were calculated by using the curves of growth by Soderblom et al. (1993). The values ΔLog N(Li) are the differences between the abundances of the binaries and the average abundances of single stars at the same color.

Name	T_{eff} (K)	T_{eff} Correct.	CCF	W(Li) Observed	W(Li) Correct.	Log N_{Li}	Log N_{Li} Correct.	ΔLog N(Li)	P_{orb} (d)	Comments
(1)	(2)	(3)	(4)	(5)	(6)	(7)	(8)	(9)	(10)	(11)
vB 1	6071	6099	1.018	103	104.9	3.07	3.13	0.13	–	
V471 Tau	5125	4752	1.017	215	218.7	2.66	2.20	$\geq$2.48	0.52	SGC, Log $N_{Li}^{Pallavic}$=2.72
vB 9	5558	–	–	$\leq$4	–	$\leq$0.80	–	$\leq$-0.89	$\geq$2555	
vB 14	7036	7063	1.007	$\leq 67^{(B1)}$	$\leq$67.5	3.28	–	∼0.06	–	Gap
BD+23°635	4528	4634	1.199	11	13.2	0.11	0.34	$\geq$0.76	2.39	SGC, Log $N_{Li}^{Pallavic}$=0.26
vB 162	5568	5700	1.724	41	$59^{(T)}$	1.96	2.31	0.13	55.1	
vB 22	5357	5542	1.373	49	67.3	1.87	2.28	0.62	5.61	
vB 23	5656	5742	1.724	44	75.9	2.08	2.52	0.21	75.648	
BD+22°669	4759	4902	1.356	–	$23^{(T)}$	–	0.95	$\geq$1.01	1.89	SCG, Log $N_{Li}^{Pallavic}$=0.89
vB 29	6091	6259	1.398	21	29.4	2.03	2.39	-0.68	32594.91	
vB 34	6534	6553	1.950	$\leq 7.9^{(B2)}$	$\leq$15.4	∼2.05	∼2.34	∼-0.08	3.08	Gap
vB 38	7227	7364	1.066	$\leq 19.6^{(B1)}$	$\leq$20.9	2.89	–	∼-0.39	2.14	Gap
vB 40	6083	6225	1.092	112	122.3	3.17	3.46	0.39	4.00	
vB 39	5659	5659	∼1.000	44	44.0	2.08	2.08	0.03	$\geq$2555	
vB 42	5394	5422	1.016	11	11.2	1.10	1.14	-0.10	–	
vB 50	5936	6024	1.048	$73^{(R)}$	76.5	2.62	2.74	-0.18	12045	
vB 52	5951	5951	∼1.000	85	85.0	2.77	2.77	-0.04	–	
vB 140	5400	5558	1.159	$\leq$3	$\leq$3.5	$\leq$0.52	$\leq$0.74	$\leq$-0.98	156.4	
vB 57	6382	6594	1.661	39	64.8	2.69	≈3.18	∼0.43	2292	Gap
vB 58	5652	5785	1.631	74	$107^{(T)}$	2.43	2.87	0.34	10106	
vB 59	6163	6176	1.005	82	82.4	2.98	3.00	-0.06	$\geq$2555	
vB 62	6188	6267	1.038	126	130.8	3.47	3.64	0.57	8.88	
vB 63	5821	5829	1.003	70	70.2	2.51	2.52	-0.02	2595.3	
vB 178	5162	5288	1.117	5	5.6	0.49	0.68	-0.09	–	
vB 69	5435	5539	1.074	11	11.8	1.15	1.28	-0.37	41.6	
vB 75	6212	6427	1.793	49	87.9	2.66	3.35	0.28	21.25	
vB 77	6335	6391	1.023	$29^{(R)}$	29.7	2.47	2.54	∼-0.45	238.9	Gap
vB 81	6475	6516	1.015	$\leq 17.6^{(B2)}$	$\leq$17.9	∼2.39	∼2.42	∼-0.37	–	Gap
vB 181	4365	4460	1.201	$\leq 30^{(D)}$	$\leq$36.0	$\leq$0.35	$\leq$0.57	–	$(11.92)^{(P_{rot})}$	SCG
vB 182	5031	5211	1.399	10	14.0	0.67	1.02	0.48	358.4	
vA677	4241	4240	∼1.000	10.7	10.7	-0.30	-0.30	$\geq$0.38	1.49	SCG
vB 91	5034	5213	1.373	$\leq$4	$\leq$5.5	$\leq$0.26	$\leq$0.59	$\leq$0.05	9131	
vB 96	5150	5237	1.775	6	10.7	0.57	0.92	0.31	4748	
J301	4540	4540	∼1.000	16.2	16.2	0.31	0.31	$\geq$0.81	1.788	SCG, Log $N_{Li}^{Pallavic}$=0.23
vB 102	5928	6032	1.060	85	90.1	2.75	2.88	-0.05	10592	
J304	4400	4488	1.159	$\leq$5	$\leq$5.8	$\leq$-0.43	$\leq$-0.24	–	60.821	SCG
vB 106	5690	5854	1.136	73	82.9	2.56	2.68	0.08	≈3652	
vB 185(p)	4529	4627	1.302	$\leq$2.3	$\leq$3.0	$\leq$-0.59	$\leq$-0.38	–	276.76	SGC, Log $N_{Li}^{Pallavic}$ $\leq$-0.43
vB 185(s)	–	4112	4.311	$\leq$ 1.2	$\leq$5.2	–	$\leq$-0.77	–	276.76	SGC
vB 142	5704	5718	1.006	54	54.3	2.26	2.27	0.04	–	
vB 113	6139	6139	∼1.000	77	77.0	2.88	2.88	-0.16	≈2555	
vB 114	5509	5565	1.032	29	29.9	1.71	1.77	0.03	$\geq$1825	
J331(p)	3921	3937	1.871	$\leq$5.0	$\leq$9.3	$\leq$-0.89	$\leq$-0.60	–	8.495	SGC
J331(s)	–	3921	2.148	11.3	24.3	-0.51	-0.16	$\geq$0.00	8.495	SGC
vB 115	5145	5228	1.068	3	3.2	0.25	0.37	-0.21	≈1460	
vB 117(p)	4596	4650	1.751	$\leq$2.4	$\leq$4.2	$\leq$-0.48	$\leq$-0.15	–	11.93	SGC, Log $N_{Li}^{Pallavic}$ $\leq$-0.25
vB 117(s)	–	4522	2.330	$\leq$1.1	$\leq$2.6	–	$\leq$-0.55	–	11.93	SGC
vB 119	6099	6225	1.077	71	76.5	2.77	2.98	-0.09	–	
vB 120	5470	5545	1.831	28	51.3	1.65	2.10	0.43	–	
vB 121	6326	6374	1.019	$\leq 116.9^{(B2)}$	$\leq$119.0	∼3.54	∼3.62	∼0.62	5.75	Gap
vB 122	6171	6212	1.840	46	84.6	2.58	3.06	-0.01	16.30	
vB 124	6356	6670	1.372	$\leq 11^{(B2)}$	$\leq$15.1	∼2.03	∼2.34	∼1.48	143.53	Gap

$(1+\alpha) = 1 + 10^{-[(V_s - V_p)/2.5]}$, correction of continuum for primary components.
(B) Boesgaard & Tripicco (1986a). The Li EW includes the weak FeI 6707.4 Å:
B1 Abundances from that paper. B2 $W(Fe{+}Li)_{BT} = W(Fe{+}Li)_T - 2.00$ mÅ.
(D) Duncan & Jones (1983).
(R) Rebolo & Beckman (1988). $W(Li)_{RB} = 1.3 \times W(Li)_T - 19.00$ mÅ.
(T) Corrected by Thornburn et al. (1993).
(P_{rot}) We have classified vB 181 as a photometric binary, and assumed that the orbital period is equal to the photometric period.

A&A manuscript no.
(will be inserted by hand later)

Your thesaurus codes are:
19(16.01.1:19.10.1:19.15.1:19.43.1

ASTRONOMY
AND
ASTROPHYSICS
5.2.2008

Lithium Abundance in Binaries of the Hyades Open Cluster*

D. Barrado y Navascués[1,2,3] **and J.R. Stauffer**[2]

[1] Depto. Astrofísica, Facultad de Físicas, Universidad Complutense. E-28040 Madrid, Spain.
[2] Harvard–Smithsonian Center for Astrophysics. 60 Garden St., Cambridge, MA 02138, USA.
[3] Fellow at the Real Colegio Complutense. 26 Trowbridge St., Cambridge, MA 02138, USA.

Received date, 13 June 1995; accepted date, 25 September 1995

Abstract. We have derived accurate and homogeneous Lithium abundances in 49 main sequence binary systems belonging to the Hyades Open Cluster by using a deconvolution method to determine individual magnitudes and colors for the primary and secondary components of the binary. The input parameters of the model are the observed Li equivalent width, the actual distance to the binary, the integrated apparent magnitude and the integrated colors of the binaries $-BV(RI)_K$.

We show that the general behavior is the same in binaries and in single stars (Li is depleted faster in K stars than in G stars and there is a deep dip for mid–F stars). However, there is a larger scatter in the abundances of binary systems than in single stars. Moreover, in general, binary systems have an overabundance, which is more conspicuous in close binaries. In fact, there is a cut–off period, which can be estimated as $P_{orb} \sim 9$ d. This value is in excellent agreement with the theoretical predition of Zahn (1994).

Table 1 is also available in electronic form at the CDS via anonymous ftp 130.79.128.5

Key words: Photometry – stars: abundances – stars: binaries: close – stars: late type

1. Introduction

The Hyades open cluster is one of the essential laboratories in Astrophysics. It is an intermediate richness cluster with an age of 6–8$\times 10^8$ yr (Mermilliod, 1981; Gilroy 1989). Due to its proximity (47.86 pc, Schwam 1991), it allows us to obtain very accurate information about a variety of topics, such as color–absolute magnitudes relations, the distance scale of the Galaxy and, therefore, the Universe, etc. It has also been essential in the determination of the time scale of a large range of phenomena.

In particular, the Hyades has been very important in the studies of the Lithium phenomenon. Li is destroyed near the bottom of the convective envelope in late spectral type Main Sequence (MS) stars. For this reason, Li is depleted with age. Since the late type members of the Hyades have known age and it is possible to obtain spectra with excellent signal–to–noise ratios (SNR), the Hyades has become a fundamental instrument to calibrate this dependence (Boesgaard 1991). In fact, the Li depletion is also characterized by a dependence on stellar mass (Cayrel et al. 1984), the presence of a deep gap for mid–F stars older than ∼100 Myr (Boesgaard & Tripicco 1986a), a dependence on metallicity (Hobbs & Duncan 1987), and an apparent dependence on rotation at least for very young stars (Marcy et al. 1985). Lately, García–López (1995) has introduced the expresion Big Lithium Gap to describe the depletion which appears for stars between G spectral type and the substellar limit, since Brown Dwarfs must not deplete Lithium (Rebolo et al. 1992). The two first peculiarities were discovered in the Hyades. Soderblom et al. (1990) showed that some Hyades stars also have overabundances compared with the average value of stars of the same color, and these excesses could be related with their binary nature. They also claim that there is a real scatter –though smaller than the scatter present in other younger clusters– in the Li abundances for stars of the same color. The presence of this scatter was confirmed in an extensive study by Thorburn et al. (1993). The role of rotation has been shown to be very important both in open clusters, such as Pleiades (Soderblom et al. 1993a) and in chromospherically active binaries (Pallavicini et al. 1992; Randich et al. 1993a,b; Fernández–Figueroa et al. 1993), but it is not totally clear how rotation affects the Li abundance.

Send offprint requests to: D. Barrado y Navascués. dbarrado@cfa.harvard.edu

Astronomy And Astrophysics, (1996), 310, 879

* Based on observations obtained at Kitt Peak National Observatory, Arizona, operated by the Association of Universities for Research in Astronomy, Inc., under contract to the National Science Foundation, USA.

Fig. 1. Normalized spectra around LiI6708 Å for (a) V471 Tau, (b) vA677, (c) J301, (d) J304, (e) vB 185 (f) vB 117 and (g) J331. Note the very broad spectral lines in the spectrum of V471 Tau and the double–lined spectra of vB 185, J331 and vB 117. All primaries except V471 Tau, vA 677 and J331 have very similar (B-V) color.

Since Li can be transported by different mechanisms inside the convective envelope or below it, it provides an important way to discriminate which mechanism is more important and to look inside the internal structure of low mass stars. These mechanisms, such as convection, meridional circulation (Charbonneau & Michaud 1988), microscopic diffusion (Michaud 1986), gravity waves (García–López & Spruit 1991; Montalban 1994), etc, have been used to explain one or more of the observed characteristics. Among these proposed theoretical explanations, the ones which involve rotation have the most potential to explain Li depletion in low mass stars. In particular, the mixing mechanisms due to the angular momentum loss (Pinsonneault at el. 1989) could explain not only the de-

pendence of the Li on age and stellar mass, but also the scatter for stars with the same age and color since the stars would have different initial angular momentum. Lately, Zahn (1994) has found that meridional circulation, which itself appears due to the angular momentum transport between the radiative core and the convective envelope, can explain the Li abundance of stars in different clusters and in particular the high Li abundance of close Hyades binaries.

Different studies have provided a large amount of data about the stellar properties of the binaries in the Hyades. At the present time, there are accurate data about the individual distances of the members (Schwan 1991; Stern 1994), extensive studies about possible faint companions of members (Mason et al. 1993) and orbital elements of binaries (Griffin et al. 1988; Stefanik & Latham 1992). With this information, we have attempted to verify whether the scatter in inferred Li abundance due to the binarity is due only to the difficulty of the analysis, or is due to other reasons, as can be the gravitational interaction between the components.

In this work, we present accurate Li abundances of binary systems belonging to the Hyades. Section 2 describes the sample and the original sources of the data. We show the method to correct the effect of the secondary star on the colors and magnitudes in Section 3 and correction of the Li equivalent width –EW(Li)– and the calculation of the abundances in Section 4. Section 5 contains the results and Section 6 the discussion and interpretation.

2. The program stars

Our sample is composed of Hyades binary systems for which it is possible to derive Li abundances. The basic data for the Hyades binaries[1] used in this work have been selected essentially from Johnson & Knuckles (1955) –the photometry–, Stern (1994) –the distances– and Thorburn et al. (1993) and this work -the Li equivalent width, EW(Li). We have compiled additional information about EW(Li) from Duncan & Jones (1983), Boesgaard & Tripicco (1986a) and Rebolo & Beckman (1988) and about the photometry from Mermilliod (1976). In total, we have analysed 52 stars belonging to 49 different binaries.

Absolute visual magnitudes for the combined components of the binary (M_V^{obs}, column 6 of Tab. 1) were calculated by using the apparent visual magnitudes given by Johnson & Knuckles (1955) and the distances given by Stern (1994) when available. For vB 9 we used the average distance modulus computed for our sample of binaries ($< m - M >= 3.41^{+0.17}_{-0.19}$), which is in excellent agreement with the value for the center of the cluster ($< m - M >= 3.40 \pm 0.04$) by Schwan (1991), based on 145 stars with high accurate proper motions.

Another four binaries do not have measured distances. However, the difference between the magnitudes of both components has been measured (see notes to Tab. 1). Therefore, it is possible to deconvolve the photometry with this information, and the solution is unique. Moreover, photometric distances were calculated for these systems. These distances are listed in Tab. 1.

Finally, one of us (JRS) obtained spectra of 7 additional late spectral type binaries -(B-V)$\geq 0.85^m$- during October 1994. The observations were made with the 4m telescope at Kitt Peak National Observatory and the red, long camera echelle spectrograph. The spectra were reduced with the routines provided within IRAF[2], using standard procedures. At our resolution (R$\sim$45000) and for rapid rotators, the LiI 6707.8 Å doublet is normally blended with FeI 6707.4 Å. We measured the total EW of the blend. Then, in order to obtain the EW(Li), we either fitted two gaussian curves to the feature or assumed a EW(Fe) from the (B-V) color index with the available data for the Hyades. The agreement between our measured or estimated EW(FeI)s with those values obtained with the empirical relation by Soderblom et al. (1993a) is good. The observed stars, visual magnitudes, signal–to–noise ratios, and EWs of different lines are given in Tab. 2. We show the normalized spectra in Fig. 1. Note the very broad spectral lines in the spectrum of V471 Tau (Fig. 1a) and the double–lined spectra of vB 185, J331 and vB 117 (Fig. 1e, Fig. 1f and Fig. 1g). All primaries but V471 Tau, vA677 and J331 have similar $(B\text{-}V)_{primary}$ color. Casual inspection of these figures shows that the lines in the double-lined spectra (those systems having a $(1{+}\alpha)$ close to 2, see Section 4.2) appear dilute because of the "extra" continuum light.

3. The Deconvolution of the photometry of binary systems

3.1. Looking for a Main Sequence

If a binary system composed by two main sequence stars is unresolved, the integrated light of the system will be both brighter and redder than the primary star alone. This phenomenon can be appreciated in Fig. 2a, where we show V vs. $(B–V)_{obs}$ for all known single members of the Hyades cluster in the range $0.20^m \leq (B–V) \leq 1.45^m$ (cross symbols) and binaries (solid and empty circle symbols). The Zero Age Main Sequence (ZAMS) from Schmidt–Kaler (1981) has been superimposed as a dotted line by using a distance modulus of 3.40^m (Schwan 1991). Since the color

[1] Hereafter, we will use the word *binary* to refer to spectroscopic, photometric and visual binaries that only have been separated by speackle interferometry, and the word *single* to refer to real single and wide visual binaries.

[2] IRAF is distributed by National Optical Astronomy Observatories, which is operated by the Association of Universities for Research in Astronomy, Inc., under contract to the National Science Foundation, USA

Table 1. Deconvolution for the Hyades binaries. The photometry is essentially from Johnson & Knuckles (1955) and the distances from Stern (1994). Spectral types for the primary and secondary components were assigned from (B-V) color indices by using the Schmidt–Kaler's (1982) ZAMS.

Star	(B-V)			Dist.	M_V			V_{obs}	Sp. Type			Binarity
	Obs.	Prim.	Sec.	(pc)	Obs.	Prim.	Sec.		Obs.	Prim.	Sec.	
(1)	(2)	(3)	(4)	(5)	(6)	(7)	(8)	(9)	(10)	(11)	(12)	(13)
vB 1[1]	0.566	0.559	1.448	43.1	4.228	4.241	9.028	7.40	–	F9 V	M1 V	VB
V471 Tau[2]	0.85	∼0.993	–	59	5.86	5.35	9.75	9.71	–	K2 V	WD	SB1
vB 9	0.708	–	–	(47.9)[b]	5.27[b]	–	–	8.67	–	G6 V	–	SB1
vB 14	0.355	0.350	1.337	38.3	2.814	2.822	8.141	5.73	–	F2 V	K8 V	SB
BD+23°635[3]	1.09	1.043	1.362	(39.9)[a]	6.375	6.573	8.322	9.38	–	K3.5 V	K9 V	SB2
vB 162[4]	0.705	0.666	0.746	49.1	4.375	4.934	5.283	7.83	–	G4 V	G9 V	SB2
vB 22[5]	0.771	0.713	0.945	50.8	4.811	5.155	6.226	8.34	G8 V	G6 V	K3 V	SB2
vB 23[6]	0.679	0.654	0.714	49.3	4.076	4.815	5.161	7.54	–	G3 V	G6 V	SB2
BD+22°669[7]	0.99	0.933	1.167	(53.1)[a]	5.859	6.190	7.310	9.48	K0	K2 V	K5 V	SB2
vB 29[8]	0.561	0.520	0.670	47.3	3.506	3.898	4.896	6.88	F8 V	F8 V	G5 V	SB
vB 34[9]	0.457	0.435	0.461	50.3	2.662	3.456	3.506	6.17	F6 V	F5 V	F6 V	SB2
vB 38[10]	0.320	0.296	0.764	47.6	2.332	2.402	5.350	5.72	Am	F0 V	G9 V	SB1
vB 40[11]	0.563	0.528	1.042	41.9	3.879	3.974	6.567	6.99	G9 V	F9 V	K4 V	VB/SB1
vB 39[12]	0.678	0.678	–	38.2	4.950	4.950	–	7.86	–	G5 V	–	SB
vB 42	0.759	0.750	1.492	52.0	5.280	5.298	9.750	8.86	G9 V	G8 V	M2 V	PhB
vB 50	0.601	0.578	1.252	45.9	4.311	4.361	7.668	7.62	G1 V	G0 V	K6 V	SB
vB 52[13]	0.597	0.597	–	43.9	4.588	4.588	–	7.80	G1 V	G0 V	–	SB?
vB 140[14]	0.757	0.708	1.134	51.2	4.973	5.131	7.130	8.94	–	G6 V	K5 V	SB2
vB 57[15]	0.491	0.466	0.530	51.2	2.914	3.542	3.989	6.46	F7 V	F6 V	F8 V	VB/SB2
vB 58[16]	0.680	0.642	0.742	46.1	4.211	4.771	5.269	7.53	G6 V	G4 V	G8 V	VB/SB2
vB 59	0.543	0.540	1.492	47.9	4.088	4.094	9.739	7.49	F8 V	F9 V	M2 V	SB
vB 62	0.537	0.518	1.194	51.0	3.842	3.883	7.443	7.38	F8 V	F8 V	K5.5 V	SB1
vB 63	0.632	0.630	1.522	46.6	4.718	4.721	11.074	8.06	G5 V	G2 V	M3 V	VB/SB1
vB 178[17]	0.837	0.794	1.295	52.7	5.421	5.541	7.868	9.03	K0 V	K0 V	K6 V	SB?
vB 69	0.746	0.714	1.315	51.5	5.081	5.159	7.983	8.64	G8 V	G6 V	K7 V	SB1
vB 75[18]	0.531	0.481	0.545	52.0	3.010	3.644	4.136	6.59	F8 V	F7 V	F9 V	VB/SB3
vB 77	0.502	0.489	1.281	47.2	3.680	3.705	7.800	7.05	F7 V	F8 V	K6.5	SB1
vB 81	0.470	0.461	1.327	52.7	3.491	3.507	8.068	7.10	F6 V	F6 V	K7 V	SB
vB 181	1.167	1.122	1.426	49.4	6.851	7.050	8.793	10.32	K	K5 V	M1 V	PhB
vB 182	0.884	0.820	1.062	53.3	5.296	5.661	6.657	8.93	–	K0 V	K4 V	SB1
vA677[19]	1.23	1.23	–	43.6	7.833	7.833	–	11.03	K6 V	K6 V	–	SB1
vB 91	0.883	0.819	1.074	53.1	5.315	5.659	6.728	8.94	K1 V	K0 V	K4 V	VB/SB1
vB 96[20]	0.841	0.811	0.881	50.1	5.011	5.634	5.910	8.51	KO IV/V	K0 V	K2 V	VB/SB1
J301[21]	1.085	1.085	–	16.7	7.306	6.789	–	8.42	dK5e	K4 V	–	SB1
vB 102	0.603	0.576	1.190	44.7	4.288	4.351	7.411	7.54	G1 V	G0 V	K5.5 V	VB/SB1
J304[22]	1.15	1.109	1.451	(47.1)[a]	6.805	6.965	8.963	10.17	K5	K5 V	M1 V	SB1
vB 106	0.669	0.623	1.089	48.6	4.527	4.666	6.829	7.96	–	G1 V	K4 V	SB1
vB 185[23]	1.1	1.046	1.299	51.6	5.907	6.587	7.886	9.47	K3 V	K3 V	K7 V	SB2
vB 142	0.665	0.661	1.501	50.3	4.832	4.832	10.304	8.34	–	G4 V	M2 V	SB1
vB 113[24]	0.549	0.549	–	41.2	4.186	4.186	–	7.26	–	F9 V	–	SB1
vB 114	0.723	0.706	1.435	49.0	5.089	5.124	8.845	8.54	–	G6 V	M1 V	SB1
J331[25]	1.41	1.400	1.421	(43.3)[a]	7.938	8.616	8.767	11.12	–	K8.8 V	K9.2 V	SB2
vB 115	0.843	0.814	1.393	50.5	5.574	5.645	8.567	9.09	–	K0 V	M0 V	SB1
vB 117[26]	1.06	1.036	1.093	48.02	6.263	6.544	6.853	9.67	K3 V	K3 V	K3 V	SB2
vB 119	0.559	0.528	1.077	44.3	3.888	3.969	6.745	7.12	–	F9 V	K4 V	SB1
vB 120[27]	0.735	0.712	0.764	52.7	4.494	5.150	5.350	7.71	–	G6 V	G8 V	VB/SB2
vB 121	0.504	0.493	1.324	52.1	3.706	3.726	8.044	7.29	–	F8 V	K7 V	SB
vB 122[28]	0.541	0.531	0.553	52.0	3.346	4.009	4.198	6.76	–	F9 V	F9 V	VB/SB2
vB 124[29]	0.497	0.428	0.783	54.2	3.057	3.319	4.879	6.27	F5/G8	F5 V	G5 V	SB2

(a) Distance estimated from the photometry.
(b) Calculated from V and $< m - M >_{binary}$=3.40
(1) ADS 2451. The photometry include the visual companion. Mason et al. (1993) estimated $\Delta V = 6.0^m$.
(2) Distance and spectral types from Strassmeier et al 1993. $(B\text{-}V)_p$ was assigned according the espectral type.
(3) $\Delta V = 1.75^m$ from Griffin & Gunn (1981). Probable triple system.
(4) $\Delta V = 0.5^m$ from Griffin & Gunn (1981).
(5) $(B\text{-}V)_p$ measured directly during the eclipse (Schiller & Milone 1987).
(6) $\Delta V = 0.35^m$ from Batten & Wallerstein (1973). It could have an additional component.
(7) $\Delta V = 1.12^m$ from Griffin et al. (1982).
(8) ADS 3135. $\Delta V = 1.0^m$ from Wickes (1975). V={7.24+8.24} from Peterson & Solenski (1987). Visual companion included in the photometry.

Fig. 2. Color–Magnitude diagrams for all known members of the Hyades cluster in the range $0.20 \leq$ (B–V) ≤ 1.45. Single stars are shown as cross symbols and binary systems as circle symbols (the solid circles represent the binaries studied here and empty circles any other binary). (a) V against (B-V). (b) M_V against (B-V). Binary systems are on average $\sim 0.5^m$ brighter than single stars. The ZAMS from Schmidt–Kaler (1981) has been superposed as a dotted line. A distance modulus of 3.4 was used in the first case. Our own MS for the Hyades cluster is shown as a solid line (see text for details).

excess $E^{\rm Hyades}_{\rm (B-V)}$=0.00 (Gilroy 1989), we do not distinguish between unreddened and reddened colors.

On average, binary systems are more than $\sim 0.5^m$ brighter than single stars. In fact, a significant number of binaries are 0.75^m brighter than the ZAMS, which is the maximum increment in brightness induced by the presence of a companion (the extreme case of two stars of equal luminosities and colors). However, there is some scatter due to different distances, since the distances for the Hyades members range from 16.7 to 72.0 pc. These extremes correspond to J301 (Borgman & Lippincott, 1983) and vB 132 (Stern, 1994).

Figure 2b shows M_V vs. (B-V)$_{\rm obs}$. In principal, the scatter introduced by the different distances has been removed in this figure (symbols are as in Fig. 2a). Only 3 binaries are above the limit of 0.7526^m (vB 75, vB 124 and BD+23°635). In fact, vB 75 and vB 124 are triple systems (Dombrowski, 1991; Griffin et al., 1985) and Griffin & Gunn (1981) found that BD+23°635 shows in its spectrum a feature that cannot be attributed to the secondary, since it does not have periodic radial velocity shifts. They conclude that it could be due to a third companion, with a long orbital period.

Based on Fig. 2b, we have catalogued vB 182, which is one of the reddest star in our sample, as a binary system. It is $\approx 0.5^m$brighter than the ZAMS, consistent with being a photometric binary (see discussion section) and inconsistent with it being a single Hyades member assuming plausible photometric errors.

Our deconvolution process requires a well defined MS with accurate photometric data. Since there is no better MS for a particular cluster than that computed from its members, we have built our own MS based on the stars belonging to the Hyades which have known distances (distances from Stern 1994). Because these distances were calculated based on the proper motions of each star, they provide accurate absolute magnitudes, removing the scatter which appears in the V vs. (B–V)$_{\rm obs}$ diagram. In addition, this MS does not contain any scatter due to evolutionary effects or due to different metallicities of the stars (e.g. see ZAMS by Schmidt-Kaler, shown as dotted line in Fig. 2b). As an illustration of the effect metallicity can have, a 1 $M_\odot$ star at the age of the Hyades cluster has $M_V = 4.383^m$ and (B-V)=0.411^m for a metallicity Z=0.001 and $M_V = 5.159^m$ and (B-V)=0.672^m for for a metallicity Z=0.020 (Schaller et al., 1992; Schaerer et al., 1993)

To select our MS, we have traced the lower envelope by hand on the M_V–(B–V)$_{\rm obs}$ diagram . Since these data are extremely accurate and they contain small errors either in the photometry –σ(V)=0.006^m, σ(B–V)=0.005^m for V $<$ 9.5– or in the distances for each member –see the discussion about the absolute magnitude errors by Schwan (1991)–, we have not considered these errors when deter-

mining the MS. The final result is shown as a solid line in Fig. 2b. The differences with the Schmidt–Kaler ZAMS can be appreciate (dotted line). Although they are not large ($\Delta M_{max} \sim 0.3^m$), these differences are extremely important when the combined photometry of a binary is calculated from its components.

3.2. The deconvolution of the photometry

We have performed a deconvolution of the photometry in order to obtain the true color of the primaries of the binaries, together with the contribution to the continuum of the secondary component. The difference between the true color for the primary and the observed color for the system can be up to 0.07^m, and the contribution to the continuum up to 50%. In principle, it is possible to reproduce the observed color and magnitude of a binary knowing its position on any color–absolute magnitude diagram, by adding the colors and magnitudes of its components. This solution is unique. It is therefore possible to reverse the process and determine the colors and magnitudes of the components based on the integrated light of the binary. Equation 1 and Eq. 2 give the color and magnitude of the primary component as a function of the observed absolute magnitude and color, as well as the magnitude and color of the secondary component:

$$M_V^p = -2.5 \text{ Log } \left\{ 10^{-M_V^{obs}/2.5} - 10^{-M_V^s/2.5} \right\} \quad (1)$$

$$(B\text{-}V)_p =$$

$$-2.5 \text{ Log } \left\{ \frac{10^{-[(B-V)_{obs}+M_V^{obs}]/2.5} - 10^{-[(B-V)_s+M_V^s]/2.5}}{10^{-M_V^{obs}/2.5} - 10^{-M_V^s/2.5}} \right\} \quad (2)$$

Seventeen binaries have an observed difference between the magnitudes of the components of the system –Δm–. In these cases, we have used this information to perform the deconvolution, matching the combined color and absolute magnitude. In some cases, there are available models for the photometry for each component, which were based on the study of the radial velocity traces of the spectral lines. We only used the differences between the magnitudes, since these models were calculated using different Main Sequences. Therefore, their results are slightly different from our own deconvolution.

The results are shown in Tab. 1: Column 1 contains either the vB (van Bueren, 1952), or DB (Bonner Durchmusterung), or J (Johnson et al., 1962) or vA (van Altena, 1969) numbers. Columns 2, 3 and 4 the (B–V) color indices for the observed system, and the colors for the primary and the secondary components, respectively. Column 5 lists the distance. Columns 6, 7 and 8 show the absolute magnitude as observed, and as calculated for the primary and the secondary components, whereas column 9 lists the apparent visual magnitude and columns 10, 11 and 12 contain the observed spectral type of the binary, and the spectral types assigned to the primary and to the secondary components based on their calculated (B–V), following Schmidt–Kaler (1981) or assigned by other studies. Column 13 gives information about the binary type.

In order to check our deconvolution method, we have performed the same procedure with other colors –namely, $(V\text{–}R)_K$, $(R\text{–}I)_K$ and $(V\text{–}I)_K$– when available. The agreement was good taking into account the uncertainties. Each CM diagram –M_V vs. (B–V), M_V vs. $(V\text{–}R)_K$, etc– allows us to obtain a continuum correction factor (1+α) –see Section 4.2– and the color index of the primary for each system. This last quantity was transformed to (B–V) color index by using different relations between these colors –$(V\text{–}R)_K$, $(R\text{–}I)_K$ and $(V\text{–}I)_K$–, and (B–V) for the single stars belonging to the Hyades Cluster. The dispersion for the continuum correction factor is 0.062 (a variation of ±6.2% in the continuum level), and the dispersion for the (B–V) color index is 0.015^m. This last value corresponds essentially to the scatter introduced by the transformation between the colors.

4. The new Li abundances

4.1. The effective temperatures

The deconvolution process (see Section 3.2) allows us to derive a more accurate (B–V) color index of the primary component, and thus, to calculate a more accurate effective temperature. We have chosen a temperature scale based on the (B–V) color. In particular, we have used the temperature scale given by Thorburn et al. (1993), in order to have the maximum consistency with that work (most of the data about EW(Li) were taken from their table 1). This temperature scale was computed from (V–K) vs. T_{eff} and (B–V) vs. (V–K) relations provide by Carney (1983), and the Cayrel et al. (1985) zero point shift. The adopted expression is:

$$T_{eff} = \frac{5040}{0.5247 + 0.5396(B-V)} \quad (3)$$

The comparison between the effective temperature derived from the integrated color of the binary (column 2 of Tab. 3) and from the calculated color of the primary (column 3 of the same table) shows that the differences are small (an average primary is ∼150 K hotter than the 'integrated star'). However, since the determination of Li abundances is extremely sensitive to the temperature, this effect is more important in general than the continuum correction (see next subsection).

Table 2. Observational data for the late spectral type Hyades binaries. The EW are not corrected for the contribution to the continuum level by the companion.

Name	V	SNR	EW(FeI6678) (mÅ)	EW(CaI6718) (mÅ)	EW(Fe+Li) (mÅ)	EW(Li) (mÅ)	Comments
(1)	(2)	(3)	(4)	(5)	(6)	(7)	(8)
V471 Tau	9.71	140	223.2	183.7	228.9	218.8	(a)
vA677	11.03	110	282.1	291.3	24.9	10.7	(b)
J301	8.42	132	247.7	260.3	32.1	16.2	
J304	10.17	85	199.5	205.5	16.5	$\leq$5.0	
vB185(p)	9.47	115	162.1	145.4	16.0	$\leq$2.3	
vB185(s)	–	–	109.1	119.6	4.6	$\leq$1.2	
J331(p)	11.12	45	119.2	133.0	–	$\leq$5.0	
J331(s)	–	–	87.2	110.9	–	11.3	(c)
vB117(p)	9.67	125	145.8	195.3	8.8	$\leq$2.4	
vB117(s)	–	–	114.8	166.4	6.9	$\leq$1.1	

pwd

(a) $<$EW(FeI6707$>_{(\mathrm{B-V})=0.85}$=13.8 mÅ.
(b) $<$EW(FeI6707$>_{(\mathrm{B-V})=1.23}$=14.7 mÅ.
(c) EW[Li(s)+Fe(p)]$^{\mathrm{measured}}$=24.3. Assumed EW[Fe(p)]$^{\mathrm{corrected}}$=EW[Fe(s)]$^{\mathrm{corrected}}$. EW[Fe(s)]$^{\mathrm{measured}}$=11.4
(p) Primary component.
(s) Secondary component.

4.2. The calculation of the Li equivalent widths for binaries

The measured EW have been corrected for the contribution to the continuum by the companion. The formula used for the correction was:

$$\mathrm{EW}_{\mathrm{corrected}} = \mathrm{EW}_{\mathrm{measured}} \times (1+\alpha) \tag{4}$$

where,

$$\alpha = 10^{-\frac{(\mathrm{V_s - V_p})}{2.5}}, \text{ primary components.} \tag{5}$$

$$\alpha = 10^{+\frac{(\mathrm{V_s - V_p})}{2.5}}, \text{ secondary components.} \tag{6}$$

We have compared the results obtained by using Eq. 4 with those obtained by using a more sophisticated expression –e.g., see Boesgaard & Tripicco (1986b), which takes into account the effective temperatures and radii to compute the contribution of each component to the local continuum around 6700 Å. The differences are quite small, with the advantage for the simpler expression that it does not need to introduce additional expressions between the radium and any other known stellar parameters of the components, such as (B–V).

The calculated continuum correction factors (1+α) are listed in column 4 of Tab. 3. As can be seen, there is a correspondence between (1+α) and the type of spectroscopic binary, when available (SB2, those stars which have spectral lines arising from both components, and SB1, where only the primary is seen). A high value of (1+α) means that both components can be seen in the spectrum and, in fact, they correspond to SB2 binaries. Batten (1973) has suggested that a secondary component 1.75$^{\mathrm{m}}$ fainter than the primary [i.e. (1+α)=1.2] should not be observed in the spectrum. Our data generally confirm this rule.

Original EW(Li)s are listed in column 5 of Tab. 3, whereas the corrected EW(Li)s are in column 6. The six EWs taken from Boesgaard & Tripicco (1986a) include the weak FeI 6707.4 Å feature. However, all are mid–F dwarf and this contribution is negligible ($\sim$ 4 mÅ). The EWs with the B1 superindex correspond to the original value of Boesgaard & Tripicco (1986a), and we also have conserved their Li abundance value. Those stars with the B2 superindex –Boesgaard & Tripicco (1986a)– and with the R superindex –Rebolo & Beckman (1988)– were corrected following Thorburn et al. (1993) in order to avoid systematic effects.

4.3. The correction of the Li abundances for binaries

We have calculated final abundances by using two different sets of curves of growth. The first set was taken from Pallavicini et al. (1987) and the $\mathrm{T_{eff}}$ range is 6500–4500 K. The input model atmospheres were those of Gustafsson et al. (1975), Bell et al. (1976) and Kurucz (1979). The second set of curves of growth was taken from Soderblom et al. (1993a) and it contains curves of growth down to 4000 K. This calculation used the model atmospheres of Bell et al. (1990). Both sets were calculated in LTE conditions. In the linear part of the curves of growth (the part that we have essentially used), the average difference between both sets is $\sim$0.07 dex, with higher abundances in the case of Soderblom's et al. (1993a) curves.

Recently, Carlsson et al. (1994) have obtained an empirical relation to correct the deviation of the LiI 6707.8 Å curves of growth in LTE from the NLTE. Since our goal

Table 3. Original abundances and corrections. The observed EW(Li) were taken primarily from Thorburn et al. (1993). The abundances commented with SCG were calculated by using the curves of growth by Soderblom et al. (1993). The values Δ N(Li) are the differences between the abundances of the binaries and the average abundances of single stars at the same color.

Name	T_{eff} (K)	T_{eff} Corr.	CCF	W(Li) Observed	W(Li) Corr.	Log N_{Li}	Log N_{Li} Correct.	Δ N_{Li}	P_{orb} (d)	Comments
(1)	(2)	(3)	(4)	(5)	(6)	(7)	(8)	(9)	(10)	(11)
vB 1	6071	6099	1.018	103	104.9	3.07	3.13	0.13	–	
V471 Tau	5125	4752	1.017	215	218.7	2.66	2.20	≥2.48	0.52	SGC, Log $N_{Li}^{Pallavic}$=2.72
vB 9	5558	–	–	≤4	–	≤0.80	–	≤-0.89	≥2555	
vB 14	7036	7063	1.007	≤67$^{(B1)}$	≤67.5	3.28	–	∼0.06	–	Gap
BD+23°635	4528	4634	1.199	11	13.2	0.11	0.34	≥0.76	2.39	SGC, Log $N_{Li}^{Pallavic}$=0.26
vB 162	5568	5700	1.724	41	59$^{(T)}$	1.96	2.31	0.13	55.1	
vB 22	5357	5542	1.373	49	67.3	1.87	2.28	0.62	5.61	
vB 23	5656	5742	1.724	44	75.9	2.08	2.52	0.21	75.648	
BD+22°669	4759	4902	1.356	–	23$^{(T)}$	–	0.95	≥1.01	1.89	SCG, Log $N_{Li}^{Pallavic}$=0.89
vB 29	6091	6259	1.398	21	29.4	2.03	2.39	-0.68	32594.91	
vB 34	6534	6553	1.950	≤7.9$^{(B2)}$	≤15.4	∼2.05	∼2.34	∼-0.08	3.08	Gap
vB 38	7227	7364	1.066	≤19.6$^{(B1)}$	≤20.9	2.89	–	∼-0.39	2.14	Gap
vB 40	6083	6225	1.092	112	122.3	3.17	3.46	0.39	4.00	
vB 39	5659	5659	∼1.000	44	44.0	2.08	2.08	0.03	≥2555	
vB 42	5394	5422	1.016	11	11.2	1.10	1.14	-0.10	–	
vB 50	5936	6024	1.048	73$^{(R)}$	76.5	2.62	2.74	-0.18	12045	
vB 52	5951	5951	∼1.000	85	85.0	2.77	2.77	-0.04	–	
vB 140	5400	5558	1.159	≤3	≤3.5	≤0.52	≤0.74	≤-0.98	156.4	
vB 57	6382	6594	1.661	39	64.8	2.69	≈3.18	∼0.43	2292	Gap
vB 58	5652	5785	1.631	74	107$^{(T)}$	2.43	2.87	0.34	10106	
vB 59	6163	6176	1.005	82	82.4	2.98	3.00	-0.06	≥2555	
vB 62	6188	6267	1.038	126	130.8	3.47	3.64	0.57	8.88	
vB 63	5821	5829	1.003	70	70.2	2.51	2.52	-0.02	2595.3	
vB 178	5162	5288	1.117	5	5.6	0.49	0.68	-0.09	–	
vB 69	5435	5539	1.074	11	11.8	1.15	1.28	-0.37	41.6	
vB 75	6212	6427	1.793	49	87.9	2.66	3.35	0.28	21.25	
vB 77	6335	6391	1.023	29$^{(R)}$	29.7	2.47	2.54	∼-0.45	238.9	Gap
vB 81	6475	6516	1.015	≤17.6$^{(B2)}$	≤17.9	∼2.39	∼2.42	∼-0.37	–	Gap
vB 181	4365	4460	1.201	≤30$^{(D)}$	≤36.0	≤0.35	≤0.57	–	(11.92)$^{(P_{rot})}$	SCG
vB 182	5031	5211	1.399	10	14.0	0.67	1.02	0.48	358.4	
vA677	4241	4240	∼1.000	10.7	10.7	-0.30	-0.30	≥0.38	1.49	SCG
vB 91	5034	5213	1.373	≤4	≤5.5	≤0.26	≤0.59	≤0.05	9131	
vB 96	5150	5237	1.775	6	10.7	0.57	0.92	0.31	4748	
J301	4540	4540	∼1.000	16.2	16.2	0.31	0.31	≥0.81	1.788	SCG, Log $N_{Li}^{Pallavic}$=0.23
vB 102	5928	6032	1.060	85	90.1	2.75	2.88	-0.05	10592	
J304	4400	4488	1.159	≤5	≤5.8	≤-0.43	≤-0.24	–	60.821	SCG
vB 106	5690	5854	1.136	73	82.9	2.56	2.68	0.08	≈3652	
vB 185(p)	4529	4627	1.302	≤2.3	≤3.0	≤-0.59	≤-0.38	–	276.76	SGC, Log $N_{Li}^{Pallavic}$ ≤-0.43
vB 185(s)	–	4112	4.311	≤ 1.2	≤5.2	–	≤-0.77	–	276.76	SGC
vB 142	5704	5718	1.006	54	54.3	2.26	2.27	0.04	–	
vB 113	6139	6139	∼1.000	77	77.0	2.88	2.88	-0.16	≈2555	
vB 114	5509	5565	1.032	29	29.9	1.71	1.77	0.03	≥1825	
J331(p)	3921	3937	1.871	≤5.0	≤9.3	≤-0.89	≤-0.60	–	8.495	SGC
J331(s)	–	3921	2.148	11.3	24.3	-0.51	-0.16	≥0.00	8.495	SGC
vB 115	5145	5228	1.068	3	3.2	0.25	0.37	-0.21	≈1460	
vB 117(p)	4596	4650	1.751	≤2.4	≤4.2	≤-0.48	≤-0.15	–	11.93	SGC, Log $N_{Li}^{Pallavic}$ ≤-0.25
vB 117(s)	–	4522	2.330	≤1.1	≤2.6	–	≤-0.55	–	11.93	SGC
vB 119	6099	6225	1.077	71	76.5	2.77	2.98	-0.09	–	
vB 120	5470	5545	1.831	28	51.3	1.65	2.10	0.43	–	
vB 121	6326	6374	1.019	≤116.9$^{(B2)}$	≤119.0	∼3.54	∼3.62	∼0.62	5.75	Gap
vB 122	6171	6212	1.840	46	84.6	2.58	3.06	-0.01	16.30	
vB 124	6356	6670	1.372	≤11$^{(B2)}$	≤15.1	∼2.03	∼2.34	∼1.48	143.53	Gap

$(1+\alpha) = 1 + 10^{-[(V_s - V_p)/2.5]}$, correction of continuum for primary components.
(B) Boesgaard & Tripicco (1986a). The Li EW includes the weak FeI 6707.4 Å:
B1 Abundances from that paper. B2 $W(Fe{+}Li)_{BT} = W(Fe{+}Li)_T - 2.00$ mÅ.
(D) Duncan & Jones (1983).
(R) Rebolo & Beckman (1988). $W(Li)_{RB} = 1.3 \times W(Li)_T - 19.00$ mÅ.
(T) Corrected by Thornburn et al. (1993).
(P_{rot}) We have classified vB 181 as a photometric binary, and assumed that the orbital period is equal to the photometric period.

is to perform a comparison between stars having the same metallicity and color, we did not apply this correction.

There are several reasons why we have used simultaneously 2 sets of curves of growths: First, we used the Pallavicini et al. (1987) curves because they reproduce fairly well the abundances obtained by Thorburn et al. (1993). However, we needed curves of growth at lower temperatures to obtain abundances for stars redder than (B–V)=$0.9^{\rm m}$. We could have used the differences between the curves at $T_{\rm eff}$=4500 K to correct those by Soderblom et al. (1993a) at lower temperatures, following Duncan & Jones (1983). However, we preferred not to make this correction because our conclusions would be unaffected by the shift and there is no reason to believe such a zero point shift would result in better abundances for the cooler stars. In fact, we studied binaries redder and bluer than (B-V)=$0.9^{\rm m}$ with two different goals: We have performed a comparative study between single stars and binary systems of the same color for those stars having (B–V)<$0.9^{\rm m}$ (and in this case we use the Pallavicini et al. curves of growth), whereas the aim of the study made with the subsample at lower temperature was to detect the presence of the Li doublet in close binaries and not in wide binaries (we use for this subsample the Soderblom et al. curves of growth).

Columns 7 and 8 of Tab. 3 show the uncorrected and corrected abundances for our sample of binary stars, respectively –where Log N(Li) = 12+Log $\left\{\frac{\rm N(Li)}{\rm N(H)}\right\}$. The first one was calculated by using the uncorrected $T_{\rm eff}$ for the binary and the measured EW(Li) –columns 2 and 5 of Tab. 3, respectively. The second one was computed by using the assigned $T_{\rm eff}$ to the primary component and the corrected EW(Li) –columns 3 and 6 of Tab. 3, respectively.

4.4. The error estimation

In order to estimate the final errors of our Li abundances, we should consider the different sources of the uncertainties, namely, the error in the measurement process of the EWs, the errors in the effective temperature scale, those given by the deconvolution calculation and, finally, those characteristic of the curves of growth.

The EWs analyzed here were taken primarily from Thorburn et al. (1993) or are original from this work. In the first case, the typical SNR is ∼200. Since most of these systems do not have a high value of v sin i and are not very cool, the determination of the continuum is quite clear, which allows one to obtain EWs with small internal errors. Thorburn et al. (1993) give $\sigma_{\rm EW}$=2.0 mÅ.

In the case of the EWs measured directly by us (V471 Tau, vA 677, J301, J304, vB 185, J331 and vB 117), the errors are sometimes more important. There are different reasons for this fact: The SNR is worse in these spectra (<SNR>∼100). Due to their lower effective temperature, new lines and molecular bands could appear close to the LiI 6707.8 Å doublet (however, in all cases we attributed the feature only to the Fe+Li blend). Finally, some of the systems have very broad lines in their spectra, because they are very rapid rotators. These phenomena lead to uncertainties in the continuum determination and blendings with other lines. We estimate the measured EW(Li) errors for V471 Tau as 25 mÅ, for vA 677 as 6 mÅ , for J301 as 2 mÅ and for the secondary of J331 as 8.2 mÅ. For the other binaries, we were only able to obtain upper limits.

As a quite conservative estimate, we assign an error of 100 K to the effective temperature.

The estimation of the errors of the deconvolution process is more complicated. A shift of +$0.1^{\rm m}$ in the locus of the Hyades MS (an estimation by eye of the error in in the location of the MS), causes differences of -$0.01^{\rm m}$ in the (B–V) color index and $0.03^{\rm m}$ in the absolute magnitude for the primaries calculated with the deconvolution process (they are hotter and fainter). This shift adds another ∼30 K to the error in the temperature and 5% the continuum correction.

In total, the average error in our abundance determination (without the error of the curves of growth) can be estimated as 0.25 dex.

5. Results

As shown in Tab. 1 and Tab. 3, we have been able to correct the colors, temperatures, EW(Li)s and Li abundances of the primary components (and in some cases the secondaries) of binary systems due to the presence of a companion. Although the correction for $T_{\rm eff}$ and EW(Li) are very small ($<\Delta T_{\rm eff}>$=150 K and $<\Delta$EW(Li)$>$=8 mÅ), these differences are enough to increase the abundances significantly for a number of stars.

Although our corrections for double-lined spectroscopic binaries are essentially equal to those performed by Thorburn et al. (1993), and they are based in the same raw data (most of them have published photometry for the components or at least magnitude differences), there are also differences (see next section). It is important to note that they did not perform any correction for the single–lined spectroscopic binaries because they found a tight correlation between the temperatures obtained from (B-V) and the total EWs of several lines of FeI and AlI. This fact allowed them to define an independent temperature scale ($T_{\rm spect}$). Since the differences between both temperatures were very small, they pointed out that it was not necessary to correct the abundances either due to reddening of the colors or the continuum contribution due to the presence of the secondary component. However, the combination of both effects is important enough to change substantially the estimated Li abundances (see Tab. 3) and the correction must be done to avoid biasing the Li abundances of the single–lined spectroscopic binaries.

Fig. 3. EW(Li) versus (B–V). Single stars are shown as crosses and binaries are shown as open circles (without the deconvolution) and solid circles (with the deconvolution) (a) Plot for the uncorrected EW(Li) data. (b) Plot for corrected EW(Li). Note that the very short–period TLBS V471 Tau is out of the frame in both cases.

6. Discussion

Figure 3a shows EW(Li) versus (B–V) for the uncorrected data. Crosses represent single stars and open circles the uncorrected data for the binaries. Despite the fact that binaries follow the same trend as single stars (the EWs decreases with the (B–V), and there is a clear gap for the mid–F stars), there are also differences: There are several cool stars with large EW(Li) –BD+23°635, BD+22°669, V471 Tau, vA 677, J301 and J331. For stars in this spectral range, Li is rapidly destroyed during the premain-sequence phase (PMS) or the first stages of the MS evolution, as has been shown by different studies in α Per, Pleiades and UMa Group (Boesgaard et al. 1988a,b; Soderblom et al. 1993a,b; García–López et al. 1994). The first two systems were studied by Thorburn et al. (1993). They interpreted their overabundances as an effect of their rapid rotation, since these systems are tidally locked binary systems –TLBS– (P_{orb}=2.39 and 1.89 d, respectively). The angular momentum transfer from the binary orbit to stellar rotation, which takes place in TLBS due to tidal effects (Zahn 1994 and references therein), inhibits the Li depletion (Pinsonneault et al. 1989; Zahn 1994). This occurs because there is less radial differential rotation, and thus less mixing between the interior and the convective envelope. The last four systems in the list above are also tidally locked (P_{orb}=0.52, 1.49, 1.788 and 8.495 d, respectively), in support of this model. In fact, their high EW(Li)s and abundances are really remarkable. The same situation appears for vB 22, vB 62 and vB 121, which have overabundances and short rotational periods (P_{orb}=5.61, 8.88 and 5.75 d, respectively). There are several alternatives to this model for the Li depletion. García–López & Spruit (1991) and Montalban & Schatzman (1994) have shown that internal gravity waves reproduce the Li depletion in F and G–K spectral type stars, respectively. On the other hand, Spruit (1987) has suggested that dynamo–induced magnetic fields, which are more intense in rapid rotators like close binaries, can inhibit the turbulent mixing. The combination of both mechanisms could also explain the overabundance we have found in TLBS. Moreover, rapid rotation can change the distribution of temperature in the stellar interior (Martín & Claret 1995) and, therefore, the Li depletion. However, all these scenarios (mixing due to radial differential rotation, gravity waves, etc) do not fit with vB 40, which has P_{orb}=4.00 d and an *uncorrected* EW(Li) similar to those of single stars at the same (B–V).

Also, there is an apparent shift in the position of the Li gap for the binaries relative to that for the single stars. The minimum EW(Li) appears at $(B–V)_{single} \approx 0.43^{m}$ and $(B–V)_{binary} \approx 0.50^{m}$. Is this a characteristic due to the binarity *per se* or it is just a bias introduced by the combined photometry of both stars in the binary systems?

Figure 3b is as Fig. 3a, except that we have plotted the corrected EW(Li) and (B–V) –solid circles– instead of the measured EW(Li) . The excesses for the TLBS still appear, but vB 40 *has an excess now*. Moreover, the pos-

sible shift of the Li gap has disappeared, adding support for the validity of our method of deconvolution.

The different behavior of Li between binaries and the single stars are more conspicuous in Fig. 4, which shows the corrected data for the Hyades stars in a Log N_{Li}–T_{eff} plane. The average Li abundance for single stars at each effective temperature is shown as a solid line and binaries are shown as solid symbols (triangles show TLBS and circles other binaries). For these corrected data, there are six notable ways in which the single and binary stars differ:

- All TLBS with T_{eff} cooler than 6500 K have overabundance (BD+23°635, BD+22°669, V471 Tau, vB 22, vB 34, vB 40, vB 62, vA 677, J301, J331 and vB 121). Note that we have not corrected the abundance of vB 38, since its high effective temperature is out of the temperature ranges of both sets of curves of growth.
- Some longer orbital period binaries also have abundances less than the average Li abundance of single stars (solid line) at the same T_{eff}.
- There are some binaries with unknown or longer orbital period larger than that of TLBS and Li overabundances (vB 58, vB 182, vB 96 and vB 120). In this case, it is not possible to relate these high abundances with rapid rotation due to tidal forces.
- The gap for mid–F stars is centered at similar temperature, but the average abundance could be higher for binaries than for single stars.
- The maximum abundance of binary stars are 0.4 dex higher than that of single stars.
- The larger scatter on the abundances is still present (note the large differences between the abundances for those systems with $T_{eff} \approx 5600$ K and also for those at $T_{eff} \approx 6300$ K).

Similar behavior has been found by Deliyannis et al. (1994) in a TLBS belonging to the older cluster M67. They found that this system has a Li abundance a factor 2 or more larger than any other M67 single stars, and a factor 3 larger than the average Li peak region.

Figure 4 also includes the Pleiades data. TLBS belonging to the Pleiades are shown as empty triangles and other Pleiades stars (single or binary) as empty circles. The Pleiades is younger than the Hyades (8.00×10^7 yr, Meynet et al. 1993) and their stars with 5500 K $\geq T_{eff} \geq$ 4000 K still have high Li surface abundances. As can be seen, the Li abundances in the cool Hyades TLBS are similar to that of the younger single stars. Thus, the Li depletion must have been inhibited during the PMS and/or the first part of the MS evolution, when a single star loses its angular momentum at a very high rate (Stauffer et al. 1994). As can be seen, the two TLBS in the Pleiades do not have a Li overabundance, as expected (Soderblom et al. 1993a; Ryan & Deliyannis 1994). This supports the idea that most of the Li depletion inhibition occurs during the MS life–time, rather than during the premain sequence phase. The data for these two systems were calculated using the corrected color and EW(Li), following the method described in Section 3.

In order to clarify the role of the binarity on the Li phenomenon, we have calculated the differences –Δ N(Li)– between the abundances of the binaries and the average abundance of single stars at the same color (solid line in Fig. 4) for the Hyades stars. The average behavior for single stars was calculated by fitting a third order polynomial for (B–V)$\geq 0.5^{m}$. This curve was extended beyond (B–V)=0.9^{m} (Teff $\leq$ 5000 K) by using the the upper limit of the abundance of those systems which are not tidally locked (dashed line).

Fig. 5 shows this difference against the orbital period for the binaries in the range $T_{eff} \leq 6500$ K. It demonstrates clearly that all binaries having $P_{orb} \leq 9$ d have significant overabundances. Zahn (1989) pointed out that binaries having $P_{orb} \lesssim 8$ d should be synchronized before their arrival on the MS. During almost the whole synchronization process and afterward, the orbital angular momentum behaves as a source of angular momentum for the rotation, replacing the angular momentum loss (Soderblom 1983). This allows the TLBS to avoid the differential rotation between the core and the convective envelope (MacGregor & Brenner 1991) and the mixing mechanism involved which is the result of it (Pinsonneault et al. 1989). Thus, their Li depletion during the PMS phase would be inhibited. In fact, if the inhibition process would take place essentially during the PMS phase, some very short binaries would retain the original Li abundance of the interstellar cloud from which the Hyades cluster would be eventually formed.

Binaries with periods $\gtrsim$ 8-9 d are not expected to arrive on the MS with their rotational periods synchronized to their orbital periods. However, binaries with orbital periods just slightly longer than this cutoff (P$\sim$10-20 d) should exchange some orbital angular momentum during PMS evolution and while on the MS. The lack of any apparent lithium enhancement in the one Hyades G dwarf binary system in this period range (vB 122, P$\sim$16.3 d) suggests that synchronization is required to prevent PMS lithium depletion, and not just "some" angular momentum transfer. It is also true, however, that some older TLBS with orbital periods larger than P_{cutoff} of the Hyades do have lithium enhancements (Barrado et al. 1994). This suggests that lithium depletion also normally occurs on the MS and that tidal synchronization even then can prevent or diminish further MS lithium depletion.

VB 181 deserves special attention. This star has not been previously classified as binary. However, its position in the CM diagram (it is 0.5^{m} brighter in absolute magnitude than a MS star of the same color) and its slightly faster than average rotation compared to stars of the same color (Radick et al. 1987), suggest that it could be a binary star (our deconvolution gives K5 V + M1 V spectral

Fig. 4. Log N(Li) against $T_{\rm eff}$. The corrected abundances and effective temperatures are shown. The average Li abundance for single stars are represented as a solid line, TLBS are shown as solid triangles, other binaries belonging to the Hyades are shown as solid circles. TLBS (open triangles) and other stars (open circles) belonging to the Pleiades are also included.

Fig. 5. Differences between the corrected Li abundance for each binary and the average Li abundance for single stars with the same temperature plotted versus the orbital period in the range $T_{\rm eff} > 6500$ K. All binaries having $P_{\rm orb} \leq 9$ d have significant overabundances.

types for both components). This star has a very high upper limit for its abundance ($EW(Li)_{corrected} \leq 36.1$ mÅ, whereas $EW(Li)_{single} \sim 10$ mÅ for (B–V)$\sim$0.80). There is another observation of this star, by Zapala (1972), who reported the presence of Li. However, Duncan & Jones (1983) only found an upper limit and specificly did not confirm the presence of Lithium. The binary system vB 117 also has a similar orbital period (11.93 d). We were also only able to get an upper limit to the abundance in this case. Since these stars could have orbital periods in the border between the synchronization during the PMS and the MS phases (we have assumed that vB 181 has an orbital period synchronized with the rotational period, P_{rot}=11.92 d), more accurate spectral observations should be made to improve their Li abundance estimates.

The most conspicuous case of Li overabundance in TLBS in the Hyades is V471 Tau. This is a system composed of a K2 V star and a white dwarf (Ruciński 1981). The orbital period is the shortest in the sample (P_{orb}=0.51118 d, Young et al. 1983). Because of our lack of knowledge of the original masses, rotation and orbital periods, and the interaction mechanisms that have taken place before and during the evolution of the former more massive star (the white dwarf) to this stage, it is only possible to speculate about the reason of this overabundance. As well as the Li depletion inhibition explained above (the very short rotational and orbital periods would have prevented any core–envelope mixing and thus the surface would have retained its primordial Li), Li could be created by spallation reactions in the envelope of the giant star which eventually evolved to white dwarf. This material could be transported to the now K2 V star via the overflow of the Roche limiting surface, following a similar mechanism of that one postulated for Walter (1995) has also pointed out that it has very cool structures on its surface. These structures could also change the Li equivalent width. Barium stars. It is also possible that our original EW(Li) has a larger than average systematic error, since the rotational broadening will blend other lines with LiI 6707.8 Å.

Three other systems are worthy of discussion. VB 9, vB 29 and vB 140 have upper limits for their abundances much lower than those expected due to their temperature. The simplest explanation would be that they are not real members of the cluster. However, their photometry agrees with Hyades membership as does, for vB 29 and vB 140, the proper motion and the radial velocity (Schwan 1991 and references therein). Both vB 9 and vB 29 have X-ray luminosities appropriate for Hyades members of that color; vB 140 however has an X-ray upper limit that is below that of typical Hyades members of its color (Stern et al. 1994).

On the other hand, vB 182 and vB 58 (and possible vB 96) have clear overabundances despite their long orbital periods. In this case, we cannot explain the overabundances by appealing to angular momentum transfer, since their separations are too wide to have tidal effects (P_{orb}=358.4 d and 27.7 yr, respectively) Are they real members? If they are, which mechanism would explain their high abundances? The photometry of the 3 systems and the radial velocity and proper motion for vB 58 and vB 96 (Schwan 1991) correspond to Hyades members. They may have been rapid rotators at Pleiades age, and for these reason they inhibit the Li depletion till that moment. After that, they have been burning Li as single stars do, but they have not lost their excess yet. This scenario suggests that they might still be relatively rapid rotators. Their slightly greater than average X–ray luminosities agree with this possibility (Stern 1994).

7. Summary

The main result of this work is the conclusion that every TLBS in the Hyades cluster have Li overabundance. This inhibition of the Li depletion would have happened essentially during the PMS and/or the first stage of the MS evolution. Further studies in tidally locked binaries in younger clusters would show exactly when the inhibition of the Li depletion takes place and the scale of the phenomenon.

Acknowledgements. This research has made use of the Simbad database, operated at CDS, Strasbourg, France. The comments by an anonymous referee have been very useful. DBN thanks the Real Colegio Complutense at Harvard University for the support as a Visiting Fellow and Charles Prosser for his help during the data gathering.

References

Barrado, D., Fernández–Figueroa, M.J., De Castro, E., Cornide, M., 1994, in: Cool stars, stellar systems, and the Sun, eds. J.–P. Caillault, APS conf. Series, vol. 64, p. 267
Batten, A.H., Wallerstein, G., 1973, Publ. Dom. Astrophys. Obs. Victoria 14, 135
Batten, A.H., 1973, in: Binary and Multiple systems of Stars, eds. J. Linsky, S. Serio, Pergamon, Oxford, UK, 13
Bell, R. A., Eriksson, K., Gustafsson, B., Nordlund, A., 1976, A&AS 23, 37
Borgman, E.R., Lippincott, S.L., 1983, AJ 88, 120
Boesgaard, A.M., and Tripicco, M.J., 1986a, ApJS 302, L49
Boesgaard, A.M., and Tripicco, M.J., 1986b, ApJ 303, 724
Boesgaard, A.M., Budge, K.G., Burck, E.E., 1988, ApJ 325, 749
Boesgaard, A.M., Budge, K.G., Ramsay, M.E., 1988, ApJ 327, 389
Boesgaard, A.M., 1991, ApJ 370, L95
Carlsson, M., Rutten, R.J., Bruls, J.H.M.L., Shchukina, N.G., 1994, A&A (in press)
Carney, B.W., 1983, AJ 88, 623
Cayrel, R., Cayrel de Stroebel, G., Campbell, B., 1985, A&A 146, 249
Cayrel, R., Cayrel de Stroebel, G., Campbell, B., Däppen, W., 1984, ApJ 283, 205
Charbonneau, P., and Michaud, G., 1988, ApJ 334, 746

Deliyannis, C.P., King, J.R., Boesgaard, A.M., Ryan, S.G., 1994, ApJ 434, L81
Dombrowski, E.G.,1991, Ph.D. thesis,, Georgia State Univ.
Duncan, D.K., Jones, B.F., 1983, ApJ 271, 663.
Eggen, O.J., Greenstein, J.L., 1965, ApJ, 141, 83
Fernández–Figueroa, M.J., Barrado, D., de Castro, E., Cornide, M., 1993, A&A 274, 373
García-López, R.J., and Spruit, H.C., 1991, ApJ 377, 268
García–López, R.J., Rebolo, R., Martìn, E.L., 1994, A&A 282, 518
García-López, R.J., 1995, in: The 9th Workshop in Cool Stars, Stellar systems and the Sun, ed. R. Pallavicini, A.D. Dupree. APS conf. Series, in press
Gilroy, K.K., 1989, ApJ 347, 835
Griffin, R.F., Gunn, J.E., 1978, AJ 83, 1114
Griffin, R.F., Gunn, J.E., 1981, AJ 86, 588
Griffin, R.F., Mayor, M., Gunn, J.E., 1982, A&A 106, 221
Griffin, R.F., Gunn, J.E., Zimmerman, B.A., Griffin, R.E.M., 1985, AJ 90, 609
Griffin, R.F., Gunn, J.E., Zimmerman, B.A., Griffin, R.E.M., 1988, AJ 96, 172
Gustafsson, B., Bell, R.A., Eriksson, K., Nordlund, A., 1975, A&A 42, 407
Heintz, W.D., 1969, A&A 1, 249
Hobb, L.M., Duncan, D.K., 1987, ApJ 317, 796
Johnson, H.L., Knuckles, C.F., 1955, ApJ 122, 209
Johnson, H.L., Mitchel, R.I., Iriarte, B., 1962, ApJ 154, 1163
Kurucz, R.L,, 1979, ApJS 40, 1
Marcy, G.W., Duncan, D.K., Cohen, R.D., 1985, ApJ 288, 259
Martín, E.L., Claret, A., 1995, A&A in press
Mason, B.D., McAlister, H.A., Hartkopf, W.I., Bagnuolo, W.G., 1993, AJ 105, 220
Mermilliod, J.–C., 1976, A&A 24, 159
Mermilliod, J.–C., 1981, A&A 97, 235
Meynet, G., Mermilliod, J.–C., Maeder, A., 1993, A&AS 98, 477
Michaud, G., 1986, ApJ, 302, 650
Montalban, J., 1994, A&A 281, 421
Montalban, J., Schatzman, E., 1995, A&A in press
Pallavicini, R., Cerruti-Sola, M., and Duncan, D.K., 1987, A&A 174, 116
Peterson, D.M., Solensky, R., 1987, ApJ 315, 286
Pinsonneault, M.H., Kawaler, S.D., Sofia, S., Demarque, P., 1989, ApJ 338, 424
Radick, R.R., Thompson, D.T., Lockwood, G.W., Duncan, D.K., Bagget, W.E., 1987, ApJ 321, 459
Randich. S., Gratton, R., Pallavicini, R., 1993, A&A 273, 194
Randich. S., Gratton, R., Pallavicini, R., 1993, A&A 283, 893
Rebolo, R., Beckman, J.E., 1988, A&A 201, 267
Rebolo, R., Martín, E.L., Maggazzu, A., 1992, ApJ 389, L83
Ruciński, S.M., 1981, Acta Astron. 31, 37
Ryan, S.G., Deliyannis, C.P., 1994, ApJ (submitted)
Schaller, G., Schaerer, D., Meynet, G., Maeder, A., 1992, A&AS 96, 269
Schaerer, D., Meynet, G., Maeder, A., Schaller, G., 1993, A&AS 98, 523
Schiller, S.F., Milone, E.F., 1987, AJ 93, 1471
Schmidt–Kaler, T., 1982 in: Landolt–Börnstein, Vol. 2b, eds. K. Schaifers, H. H. Voig. Springer, Heidelberg
Schwan, H., 1991, A&A 243, 386
Soderblom, D.R., 1993, ApJS 53, 1
Soderblom, D.R., Oey, M.S., Johnson, D.R.H. Stone, R.P.S., 1990, AJ 99, 595
Soderblom, D.R., Jones, B.F., Balachandran, S., Stauffer, J.R, Duncan., D.K., Fedele, S.B., Hudon., J.D, 1993, AJ 106, 1059
Soderblom, D.R., Stauffer, J.R, Hudon, J.D., Jones, B.F., 1993, ApJS 85, 315
Spruit, H.C., 1987, in: The INternal Solar Angular Velocity: Theory and Observations. eds. B.R. Durney & S. Sofia, Reidel, Dordrech. p. 185
Stauffer, J.R., 1994, in: Cool stars, stellar systems, and the Sun, eds. J.–P. Caillault, APS conf. Series, vol. 64
Stefanik, R.P., Latham, D.W., 1992, in: Complementary Approches to Double and Multiple Star Research, IAU Coll. 135, eds. H.A. MacAlister and W.I. Hartkopf, APS conf. Series, vol. 32
Stern, R.A., 1994, private communication.
Strassmeier, K.G., Hall, D.S., Fekel, F.C., Scheck, M., 1993, A&AS 100, 173
Thorburn, J.A., Hobbs, L.M., Deliyiannis, C.P., Pinsonneault, M.H., 1993, ApJ 415, 150
van Altena, W.F., 1969, AJ 74, 2
van Bueren, H.G., 1952, Bull. Astron. Inst. Neth. 11, 385.
Walter, F.M., 1995, in: Stelar Surface Structure, IAU Symp. 176. eds. K.G. Strassmeier. In press
Wickes, W.C., 1975, AJ 80, 1059
Young, A., Klimke, A., Africano, J.L., Quingley, R., Radic, R.R., van Bueren, D., 1983, ApJ 267, 655
Zahn, J.–P., 1989, A&A 220, 112
Zahn, J.–P., 1994, A&A 288, 829
Zapala, R.R., 1972, ApJ 172, 57

This article was processed by the author using Springer-Verlag LaTeX A&A style file *L-AA* version 3.

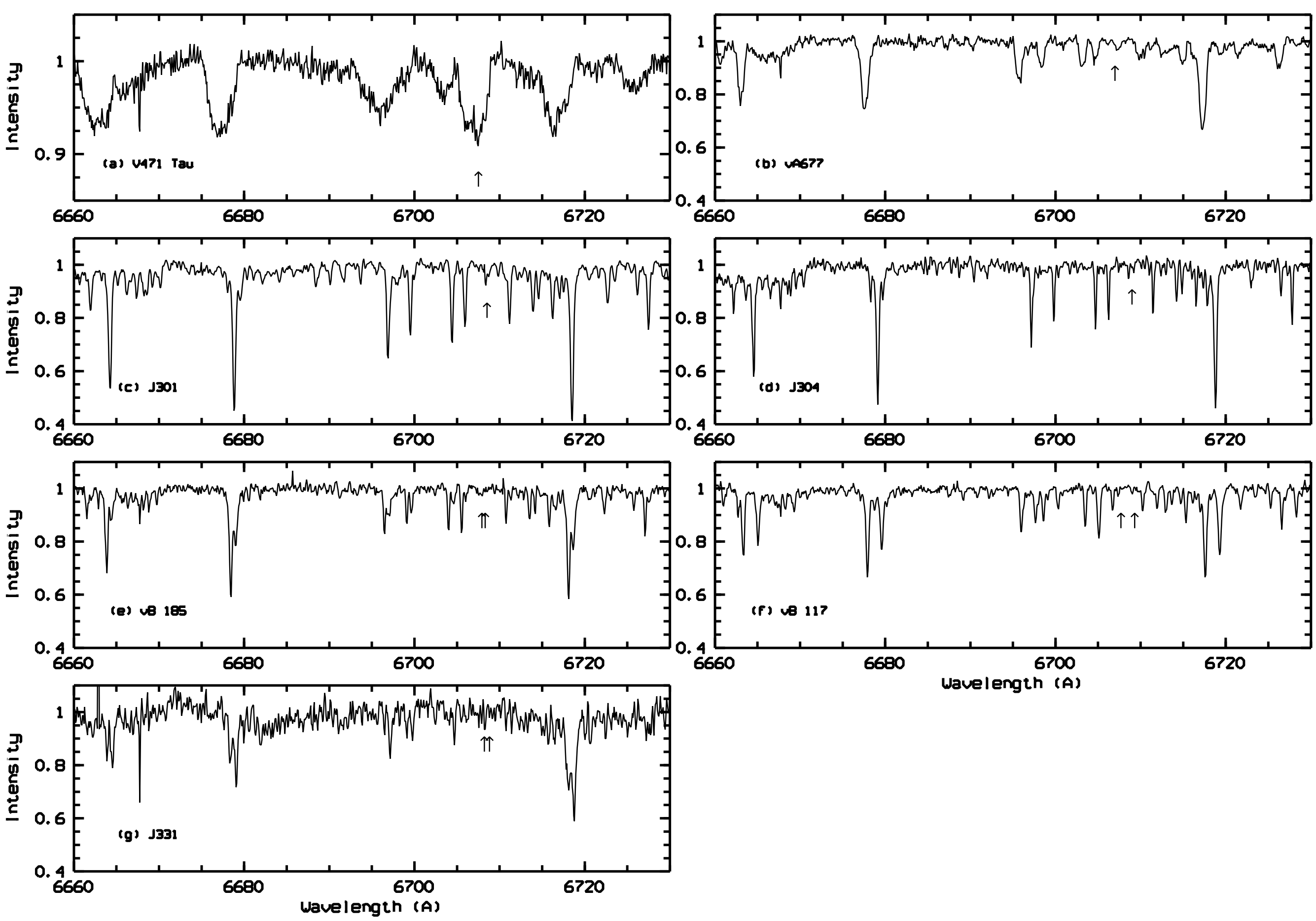

(a) V471 Tau
(b) vA677
(c) J301
(d) J304
(e) vB 185
(f) vB 117
(g) J331
Intensity
Wavelength (A)
6660
6680
6700
6720

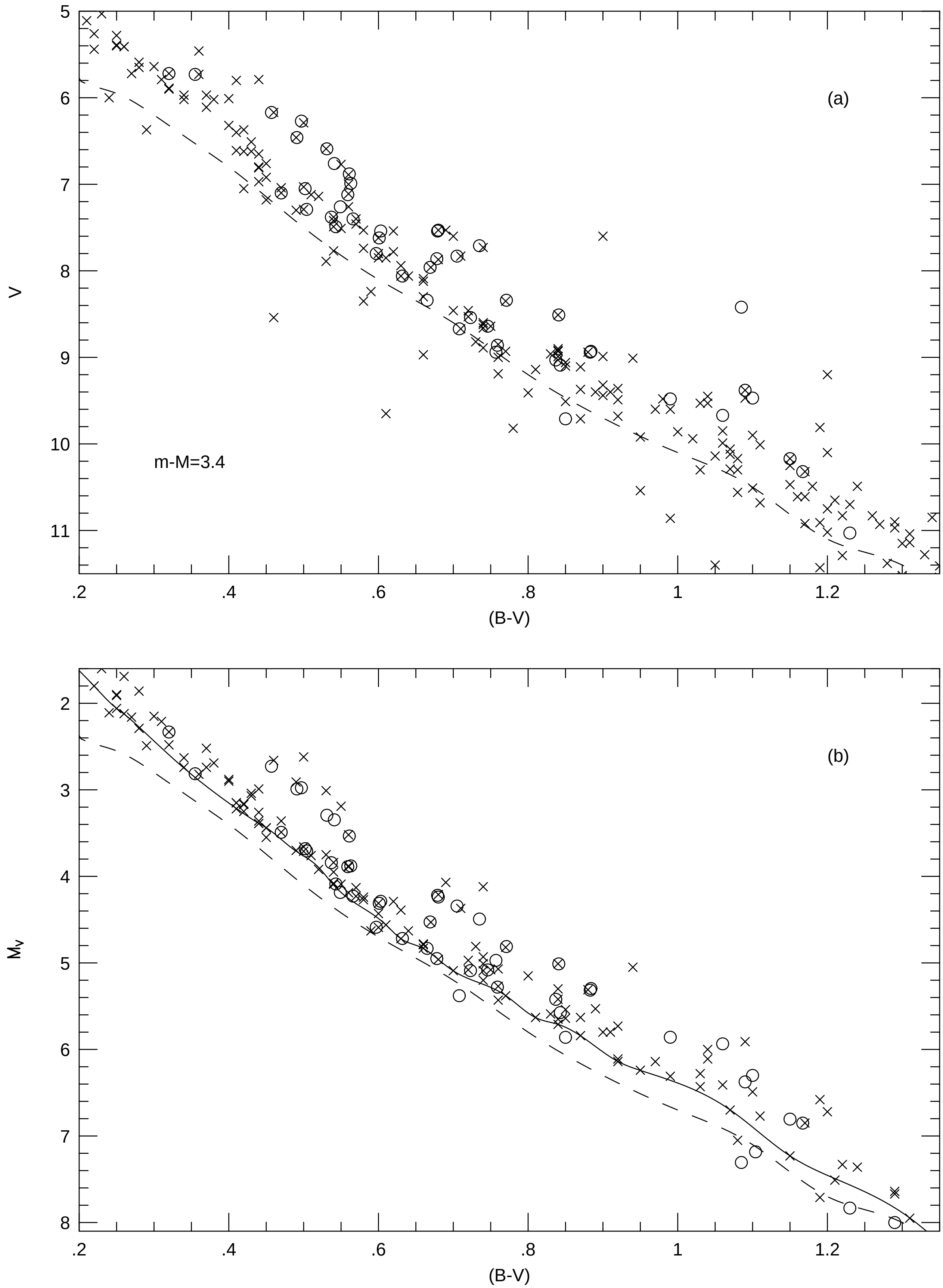
(a)
m-M=3.4
V
(B-V)
(b)
M_V
(B-V)

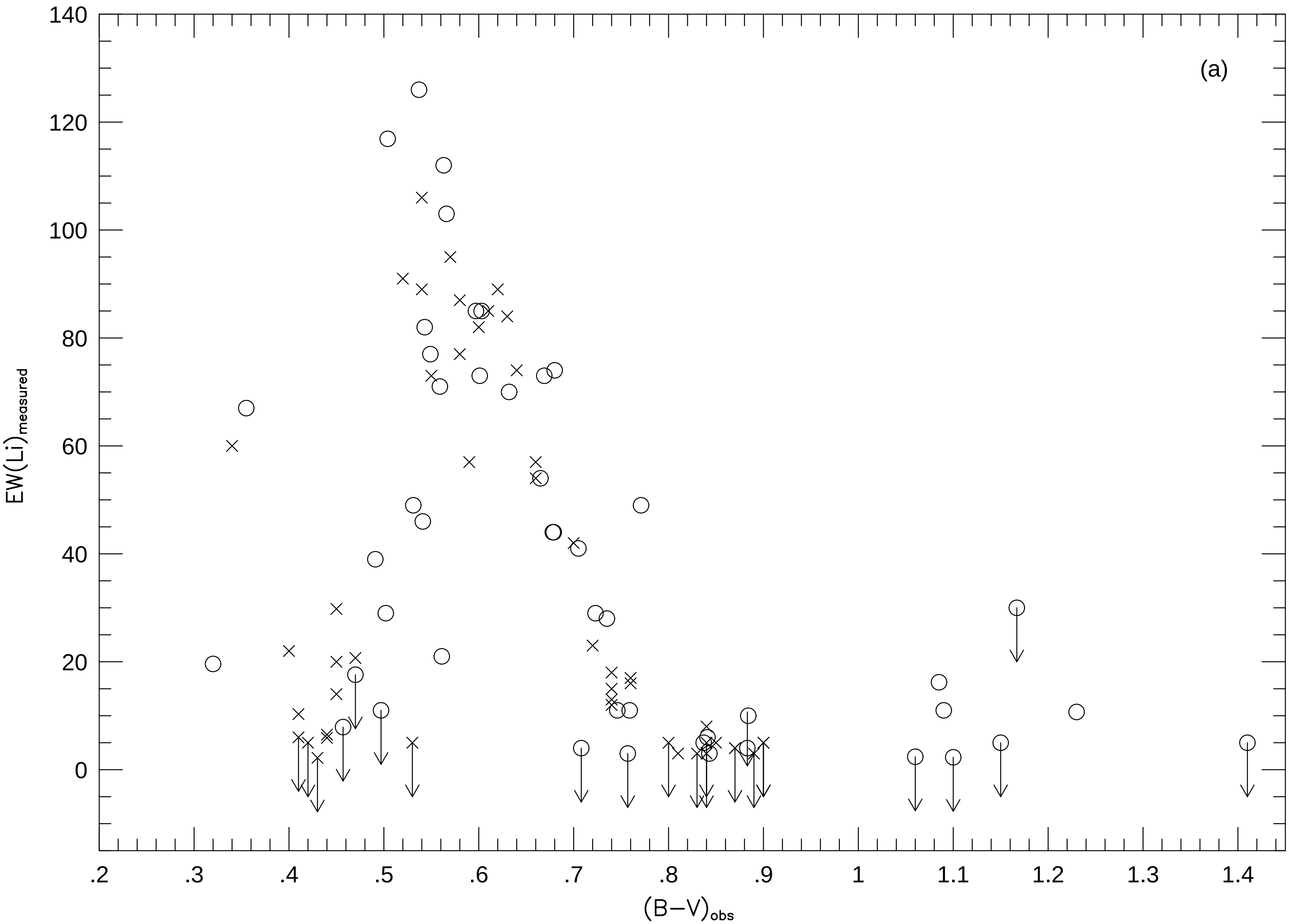
(a)
EW(Li)measured
140
120
100
80
60
40
20
0
.2
.3
.4
.5
.6
.7
.8
.9
1
1.1
1.2
1.3
1.4
(B−V)obs

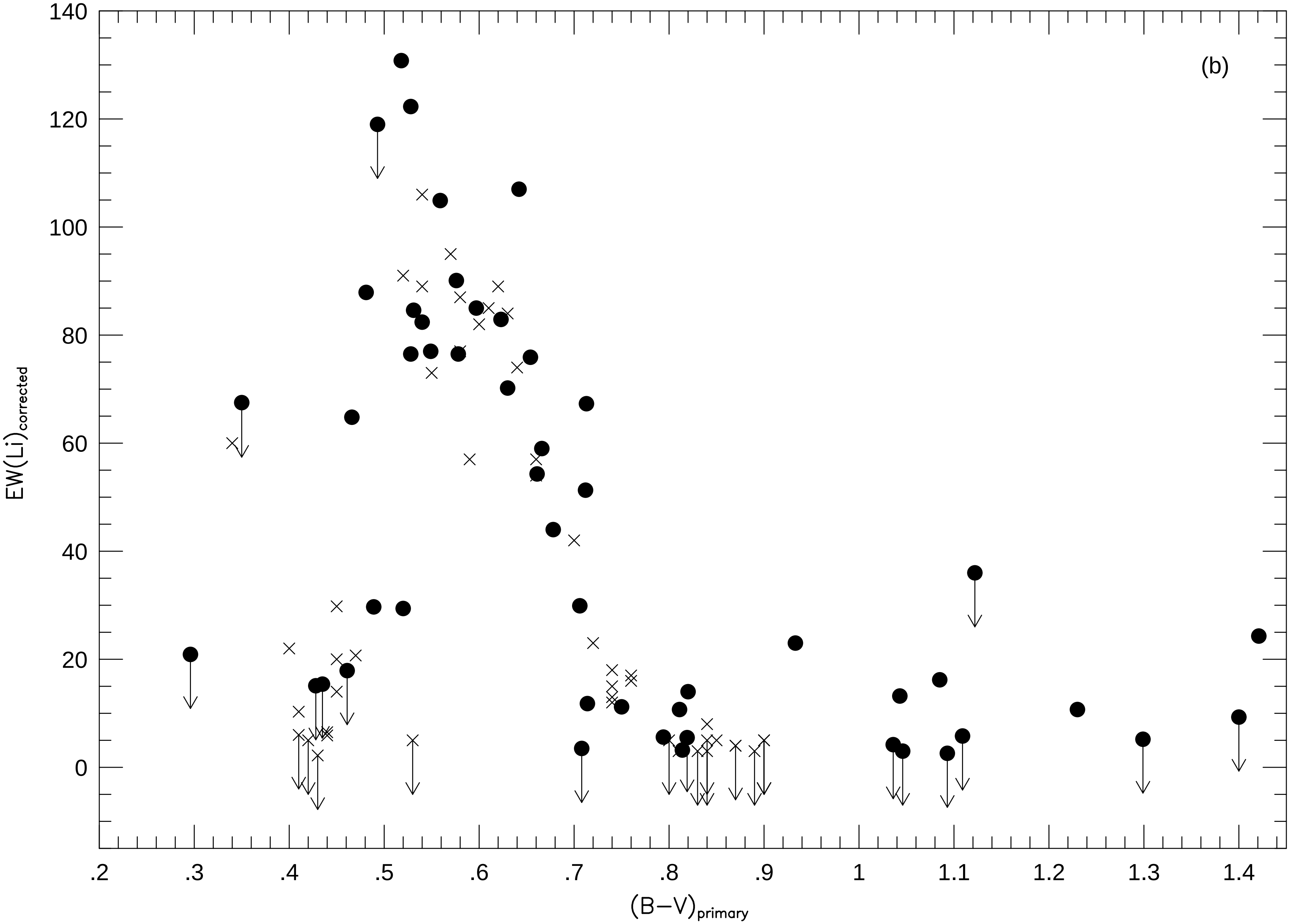

(b)
EW(Li)$_{corrected}$
(B−V)$_{primary}$
140
120
100
80
60
40
20
0
.2
.3
.4
.5
.6
.7
.8
.9
1
1.1
1.2
1.3
1.4

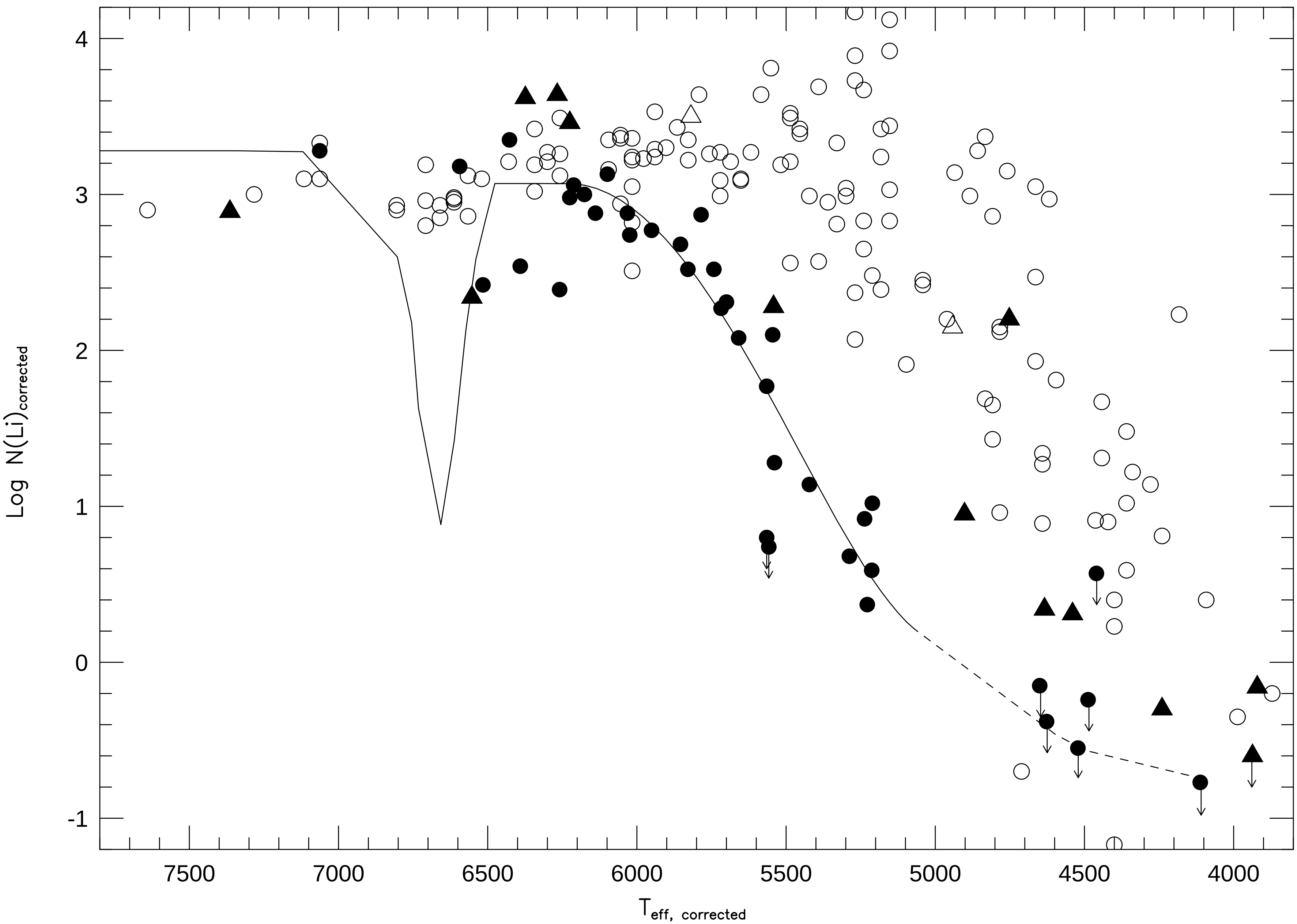

Log N(Li)corrected
4
3
2
1
0
-1
7500
7000
6500
6000
5500
5000
4500
4000
Teff, corrected

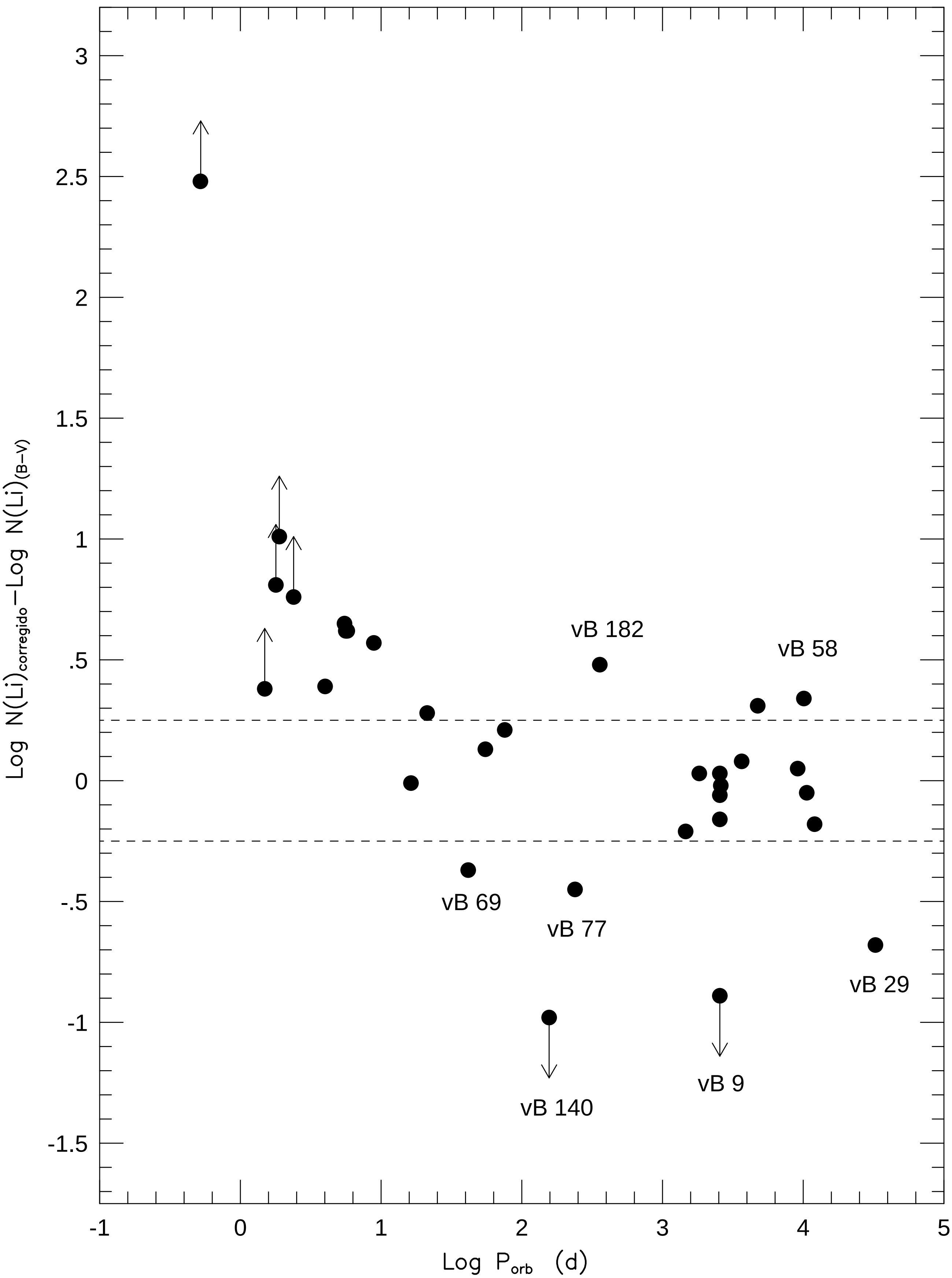

vB 182
vB 58
vB 69
vB 77
vB 29
vB 9
vB 140
Log N(Li)corregido−Log N(Li)(B−V)
Log Porb (d)